

A recipe for exotic continental fragment formation: automated data analysis of rift models

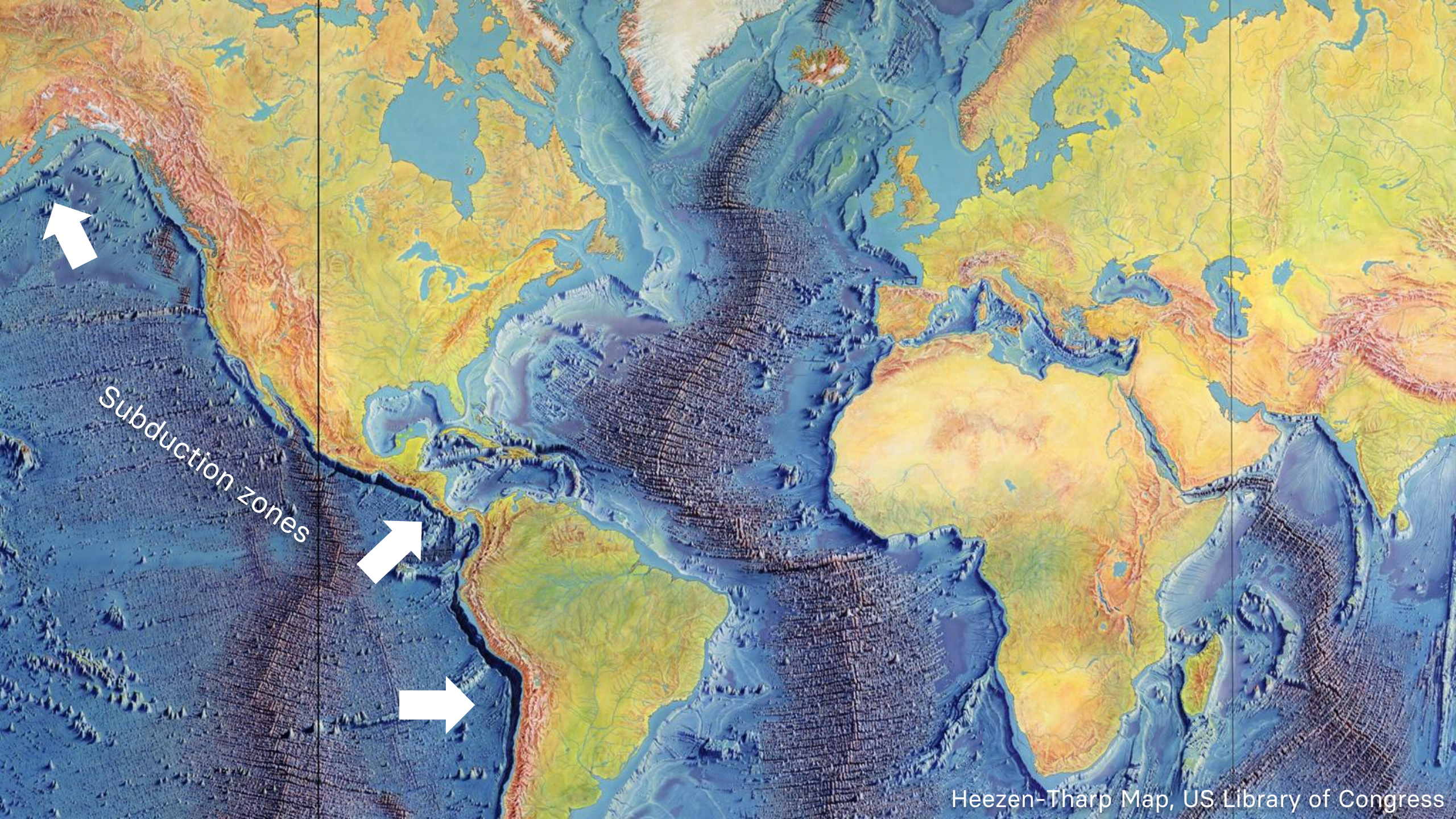
Alan Yu, Erkan Gun, Ken McCaffrey, Phil Heron



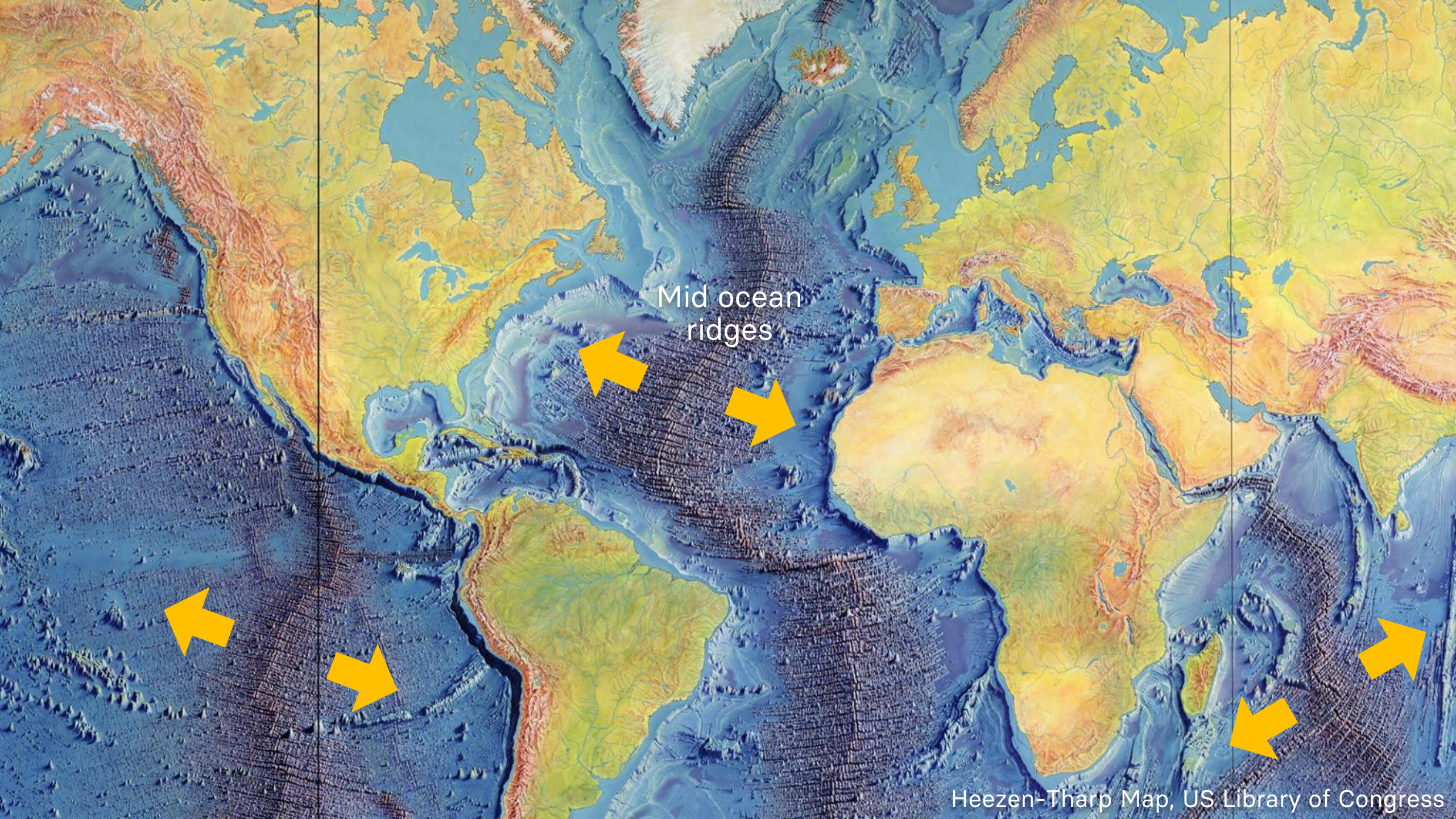
Heezen-Tharp Map, US Library of Congress



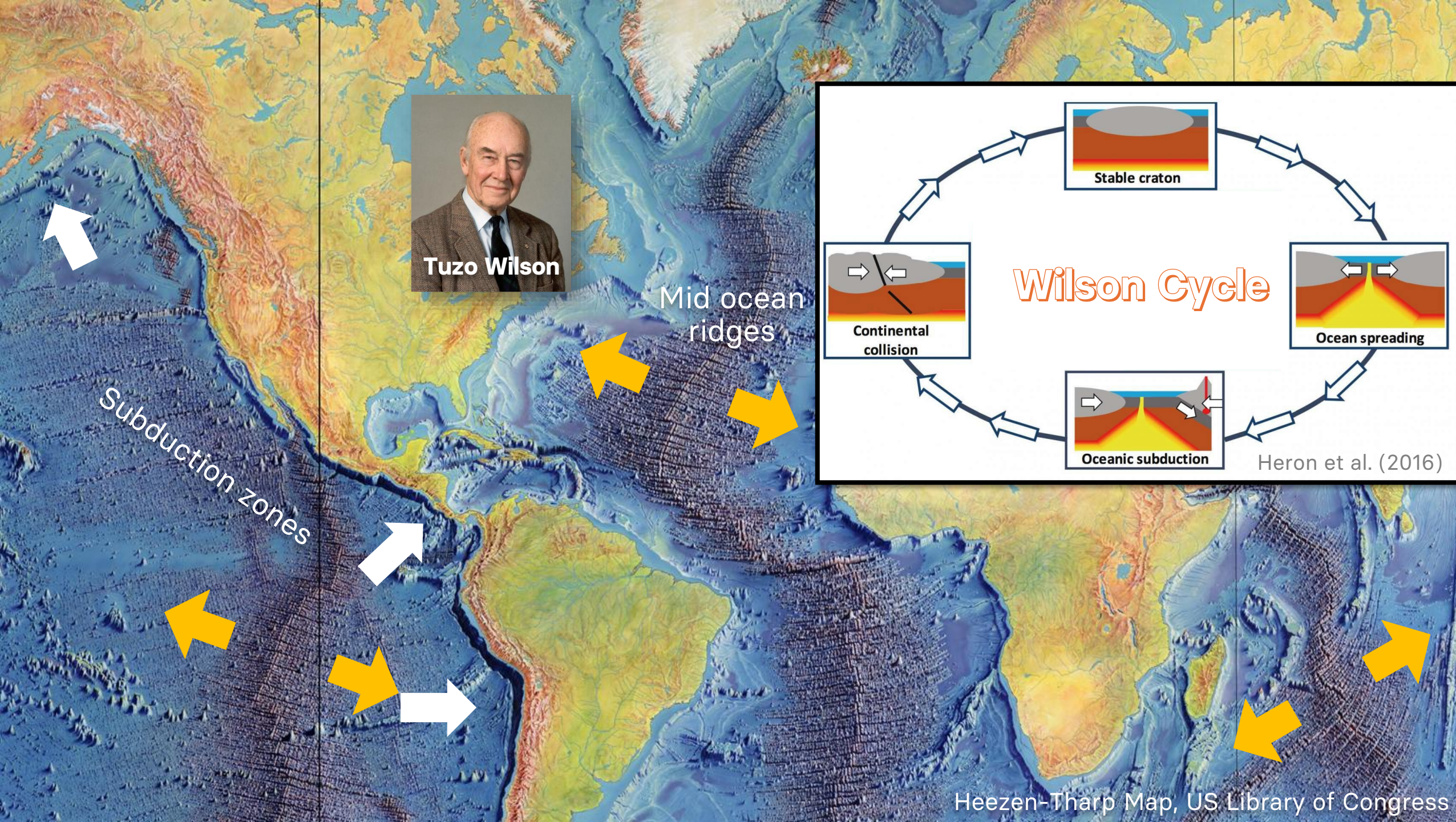
Heezen-Tharp Map, US Library of Congress



Heezen-Tharp Map, US Library of Congress

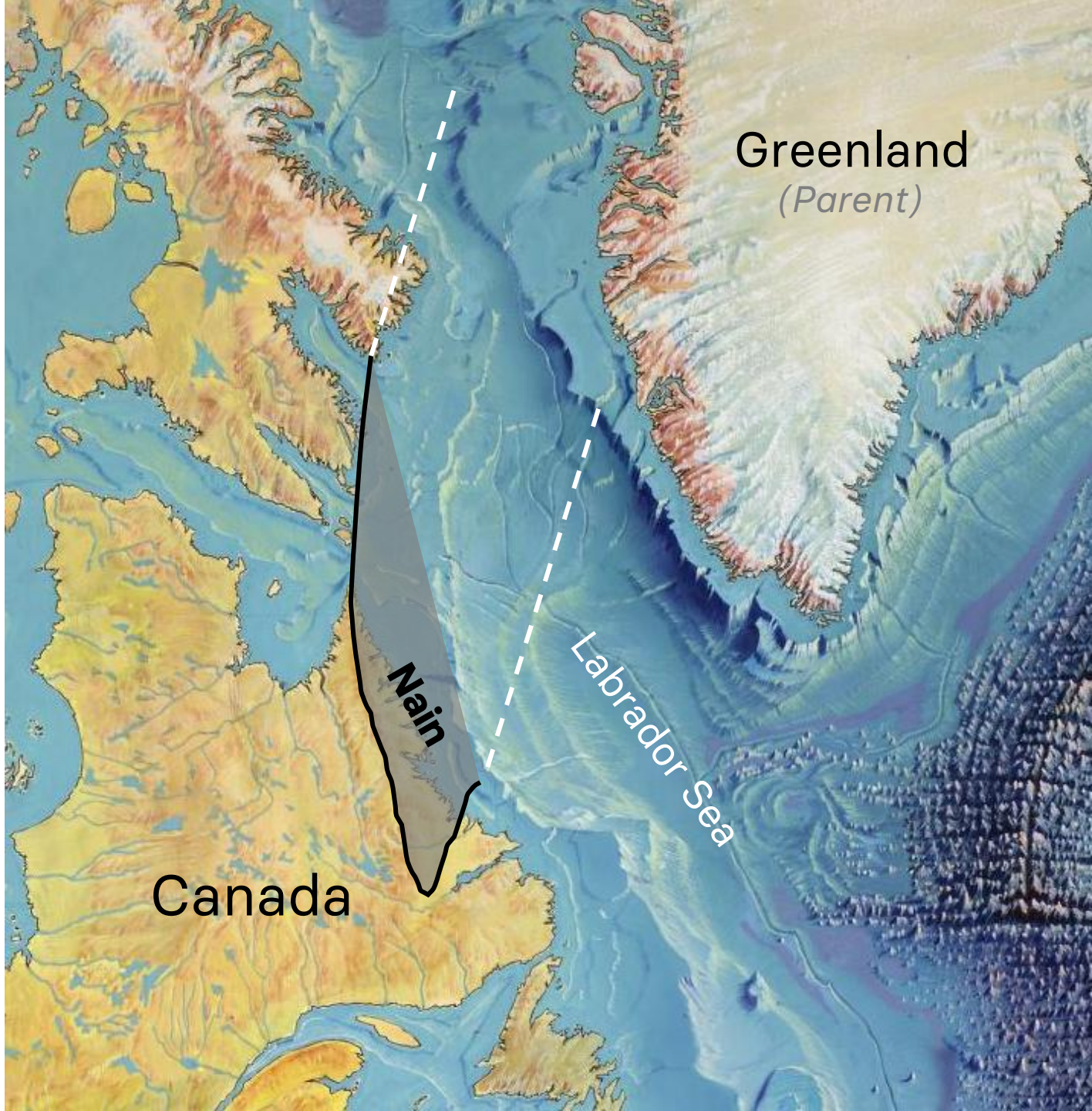


Heezen-Tharp Map, US Library of Congress



Continental fragment

- The general view of Wilson Cycle does not explain more **nuanced** tectonic scenarios.
- The opening of the Labrador Sea left a piece of "Greenland" (the **Nain Province**) in Eastern Canada.
- Continental fragment is **a small piece of continent** separated from its parent plate.
- They share the **same geological history** prior to separation.



Continental fragment

North Atlantic Ocean

Nain Province

Lewisian Complex

South Atlantic Ocean

São Luís Craton

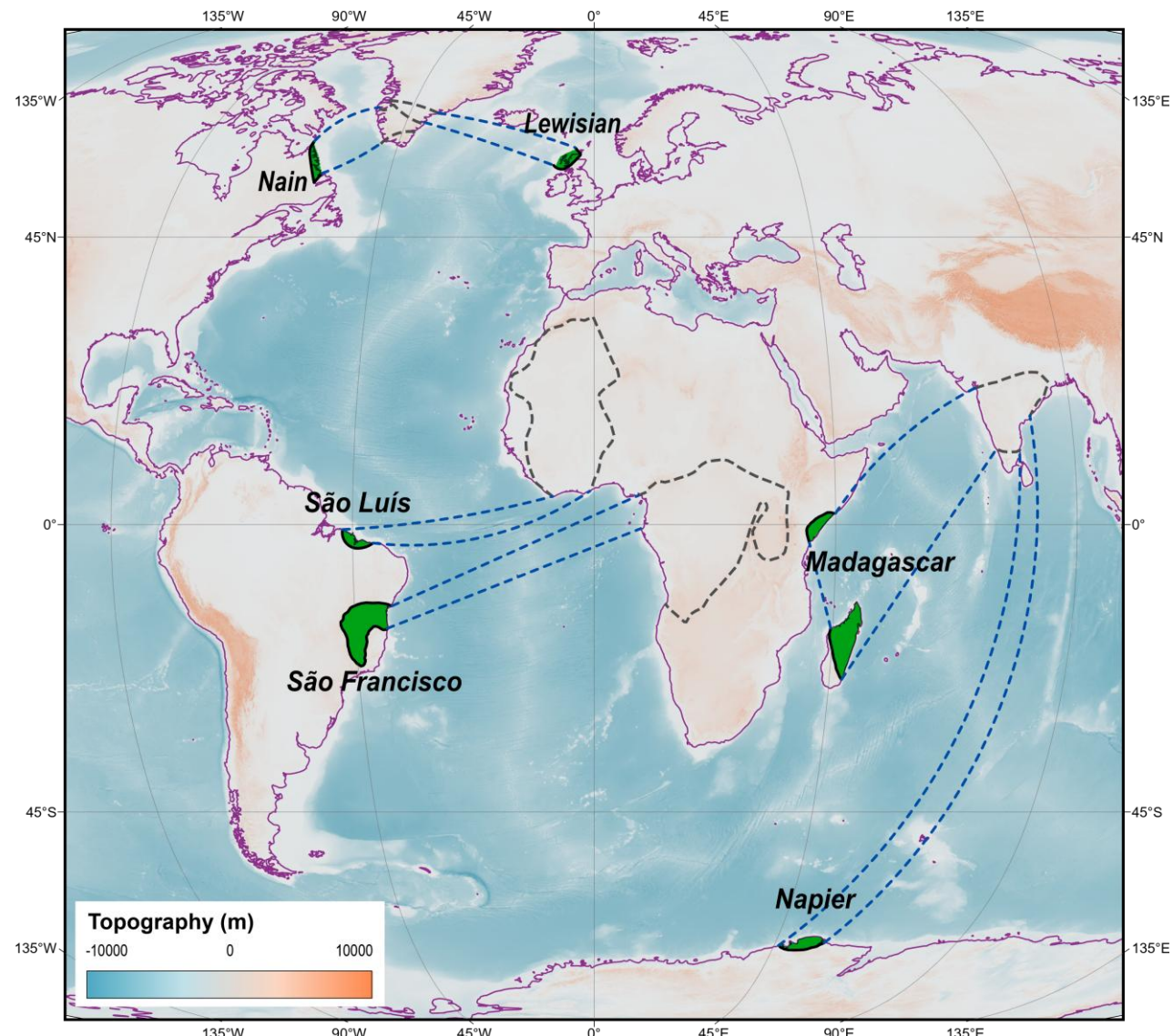
São Francisco Craton

Indian Ocean

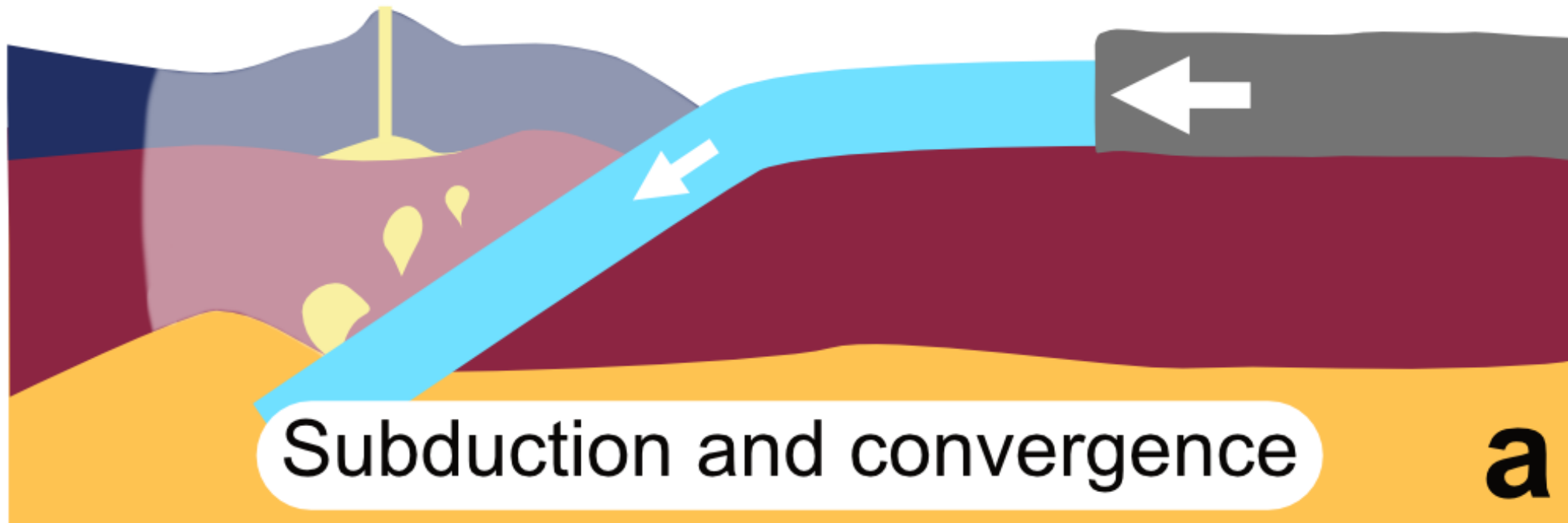
Madagascar

Napier Complex

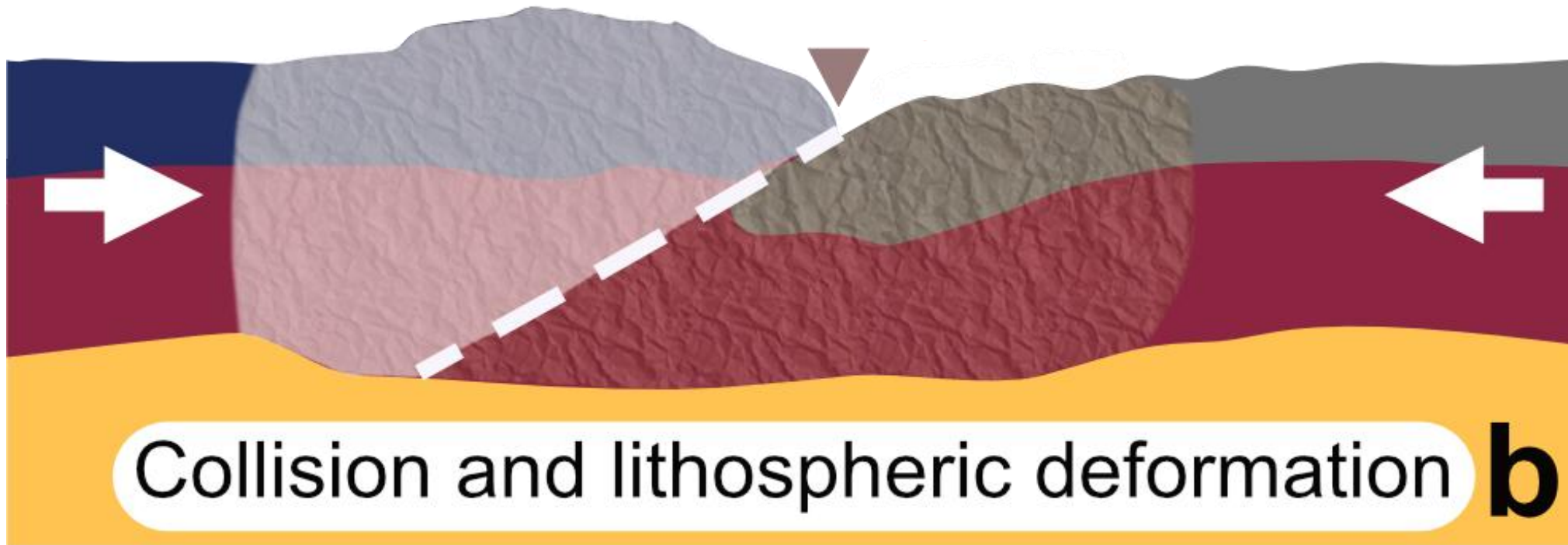
How did they form?



Wilson Cycle



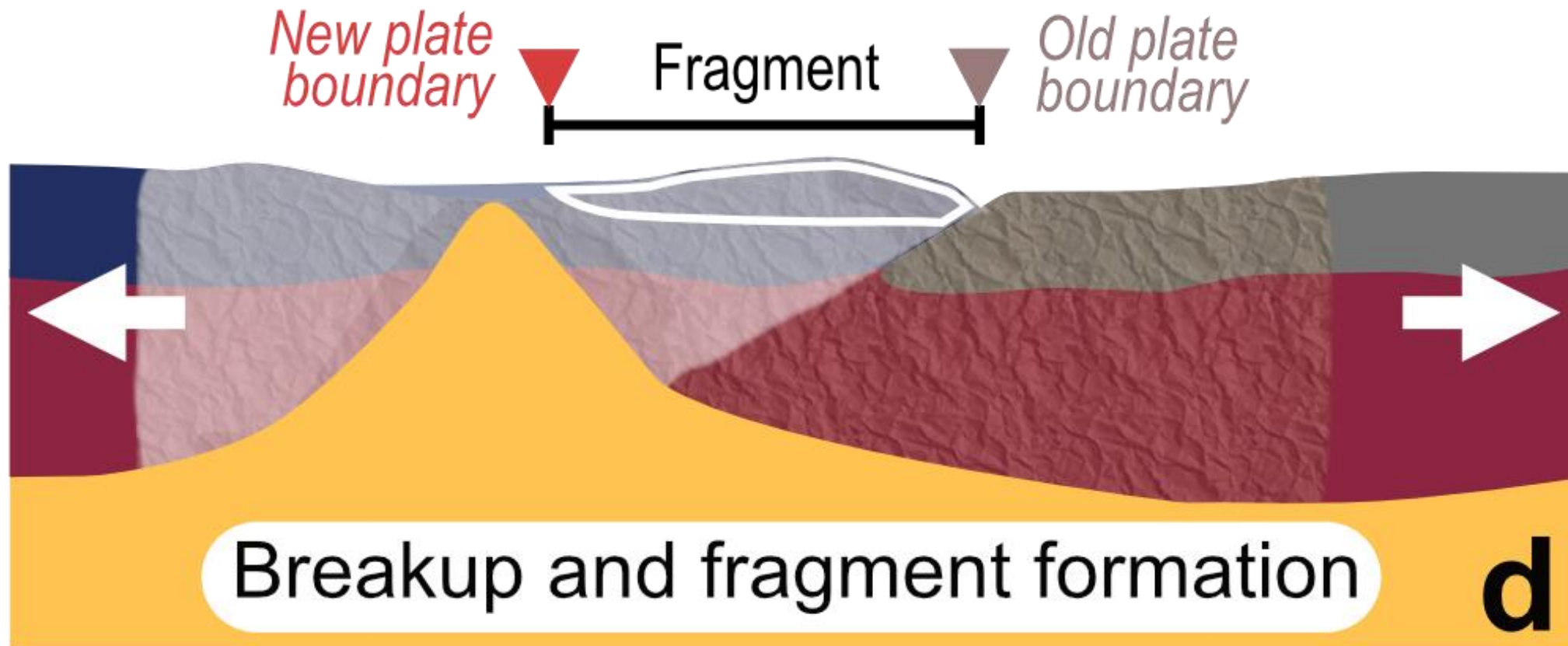
Wilson Cycle



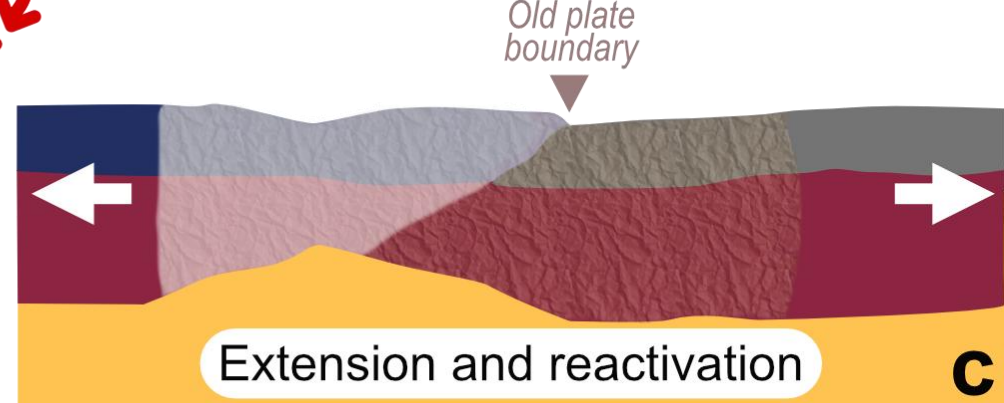
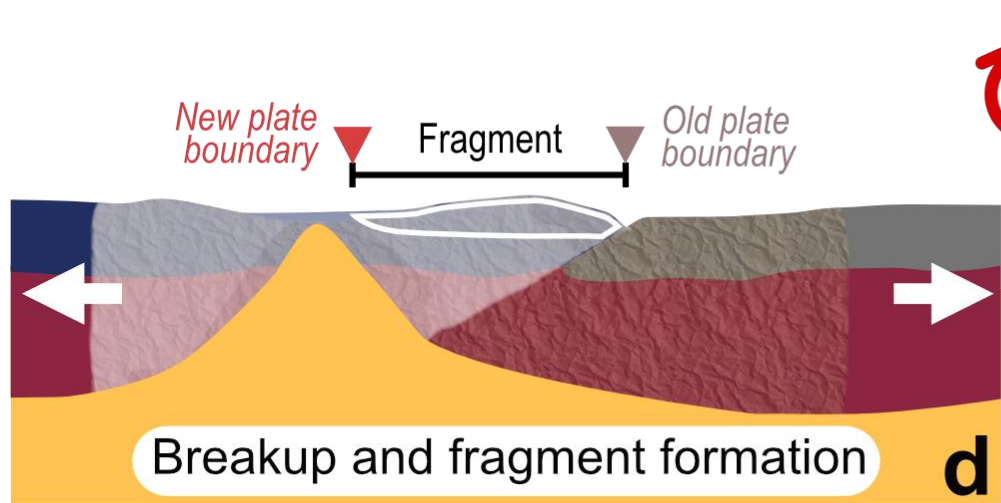
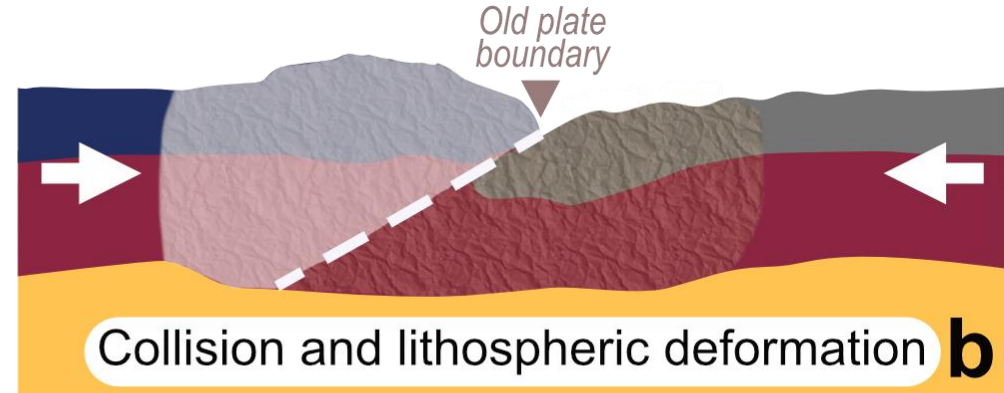
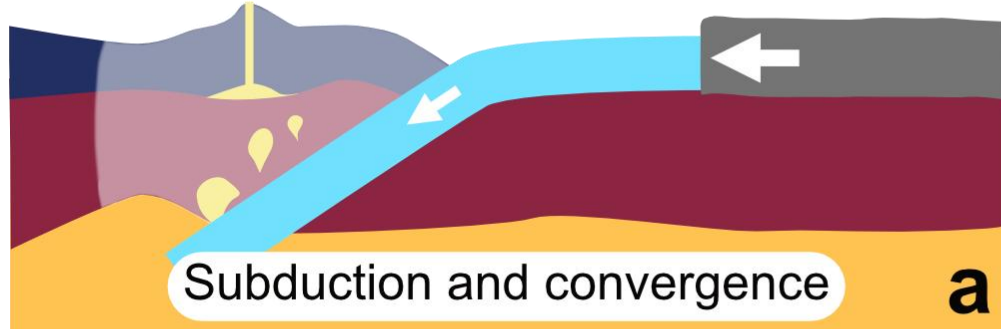
Wilson Cycle



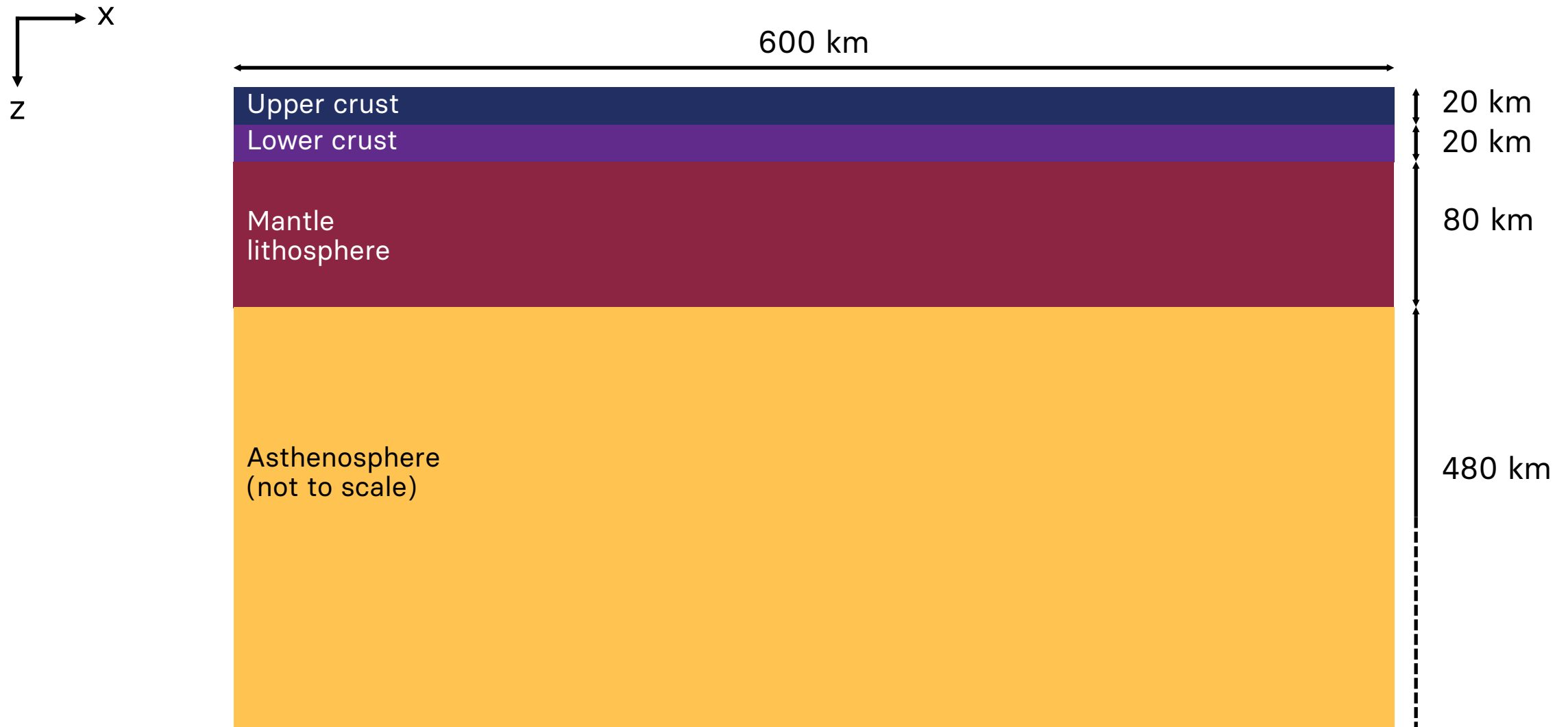
Wilson Cycle



Wilson Cycle



Model setup



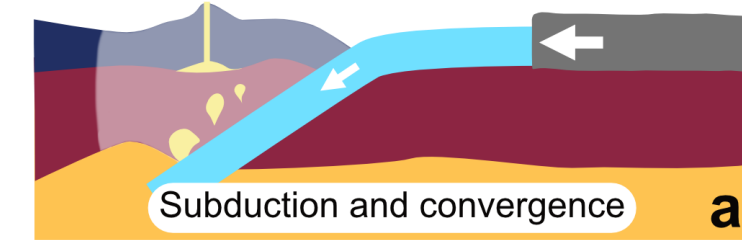
Model setup

X
Z

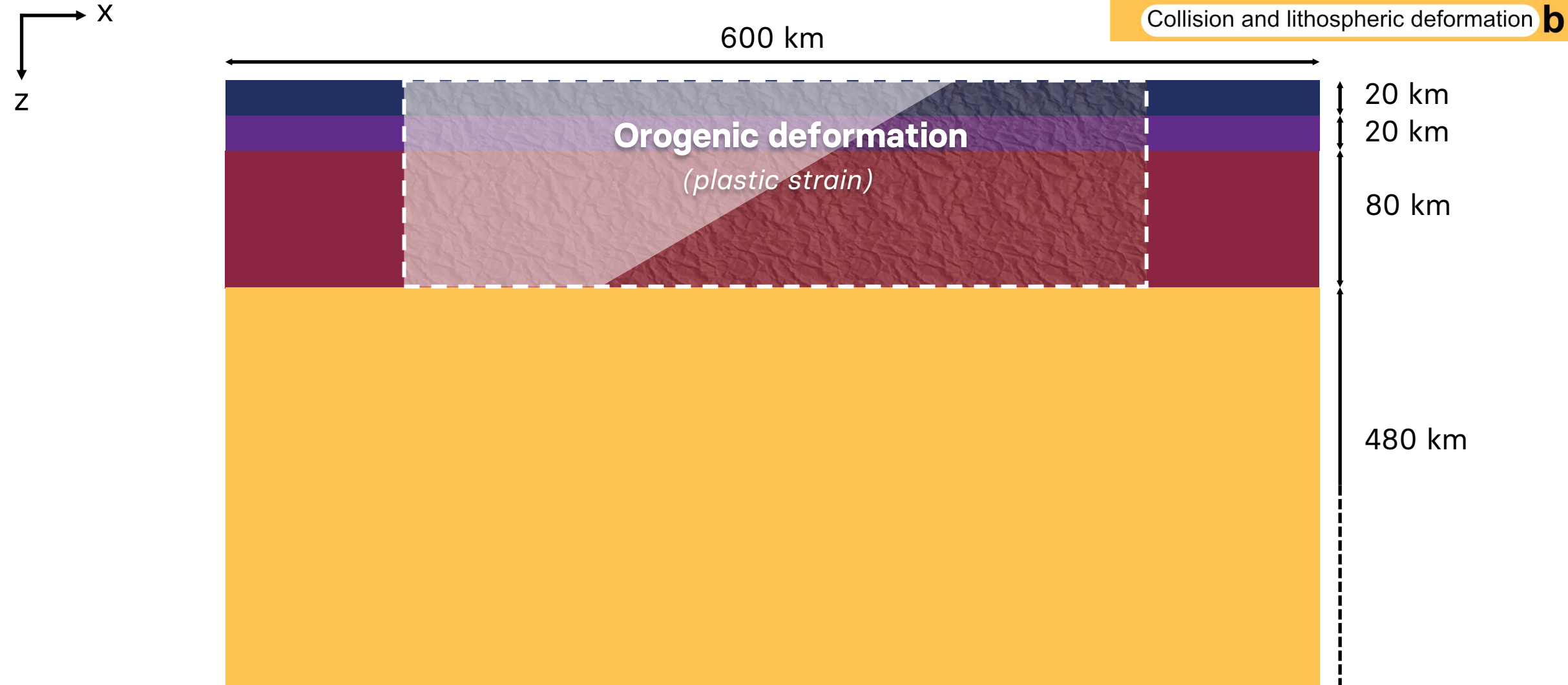
600 km



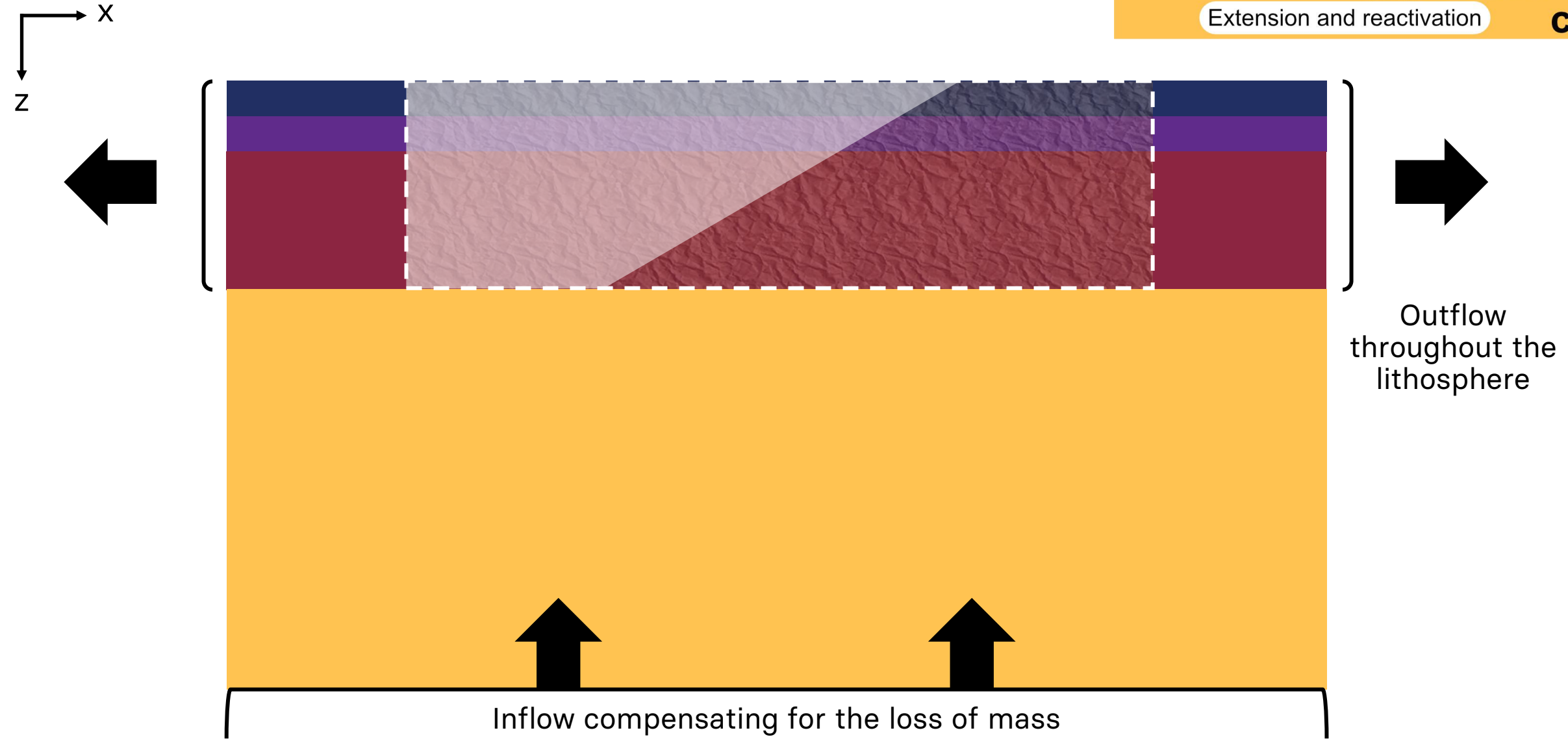
$$f = \frac{\eta_{\text{Upper plate margin}}}{\eta_{\text{Lower plate margin}}}$$



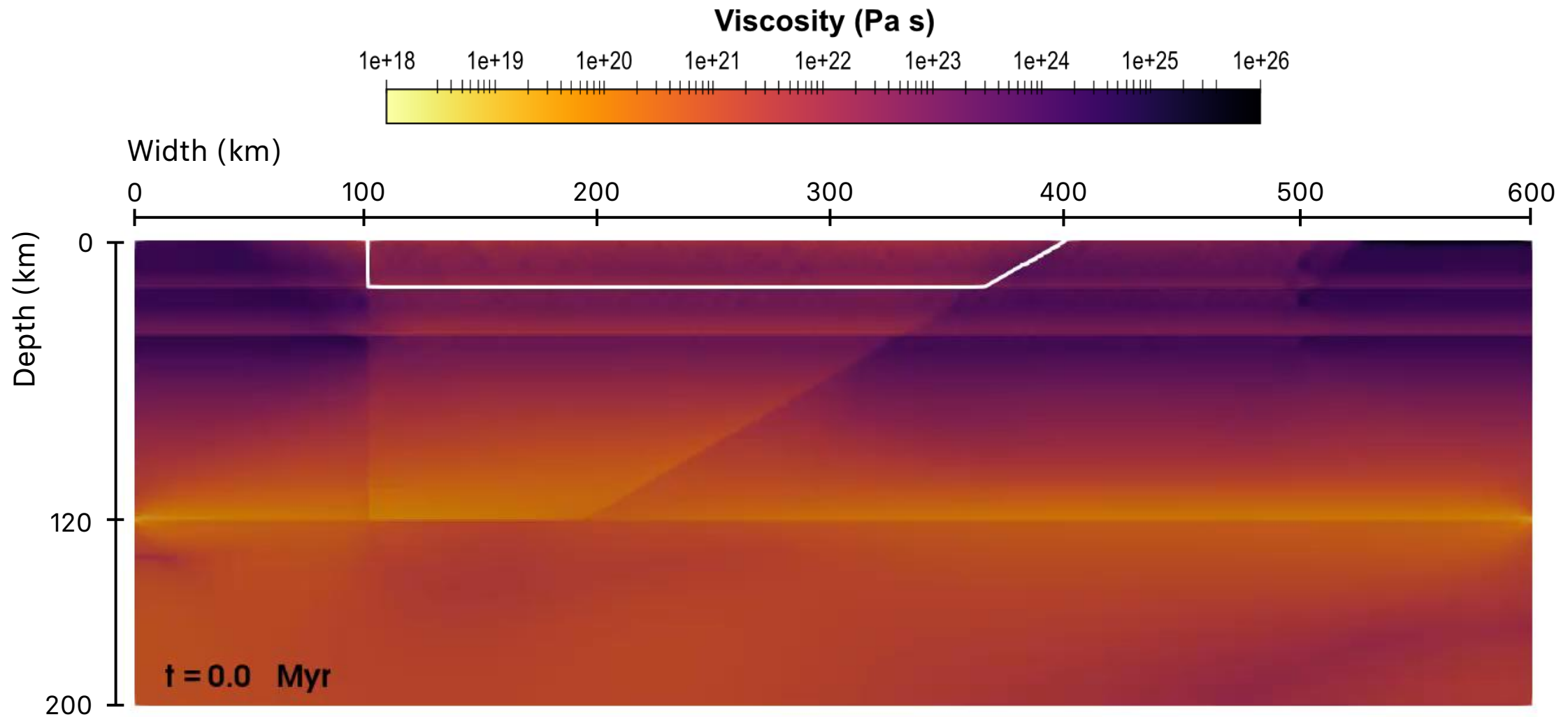
Model setup



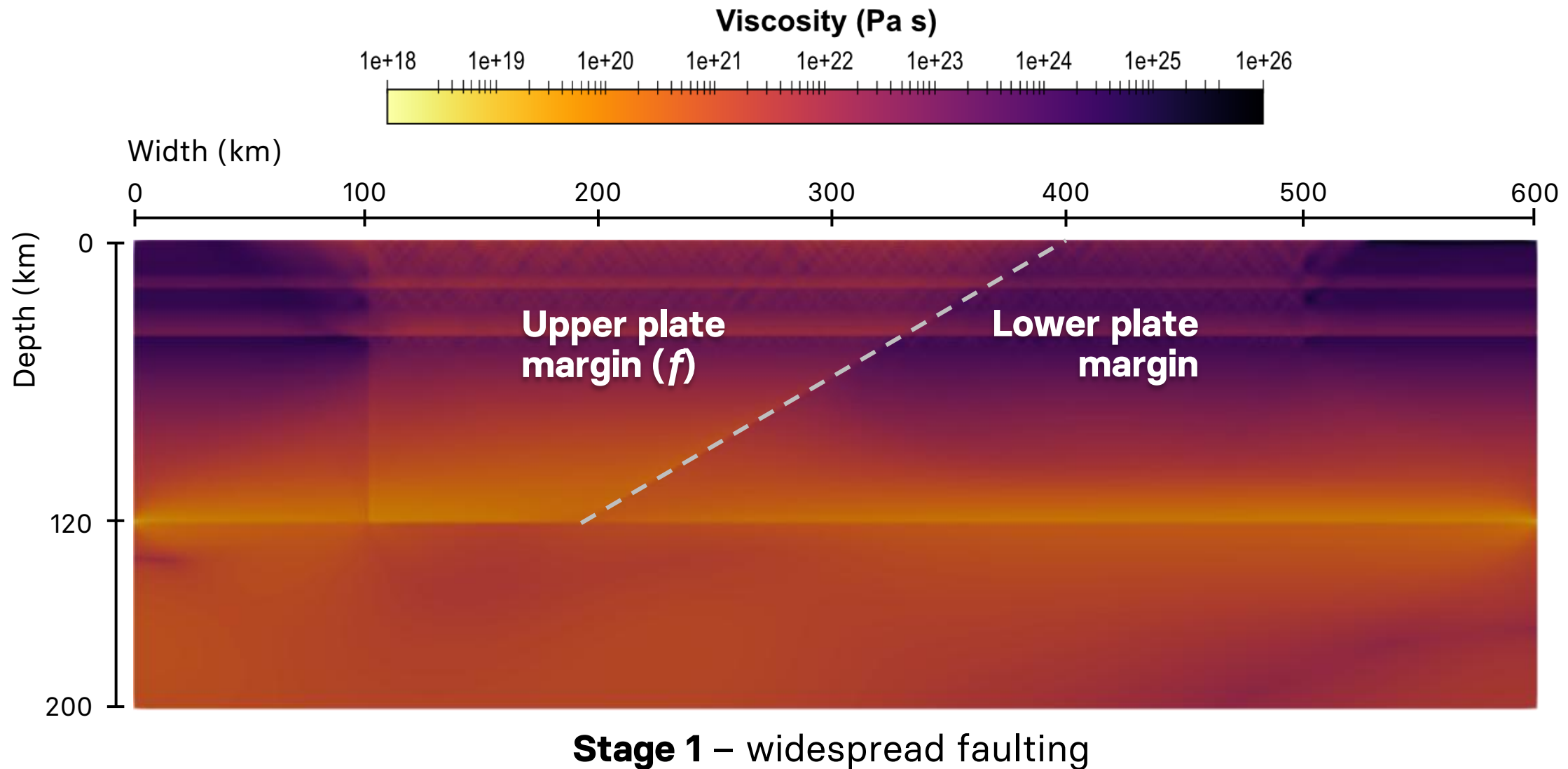
Model setup



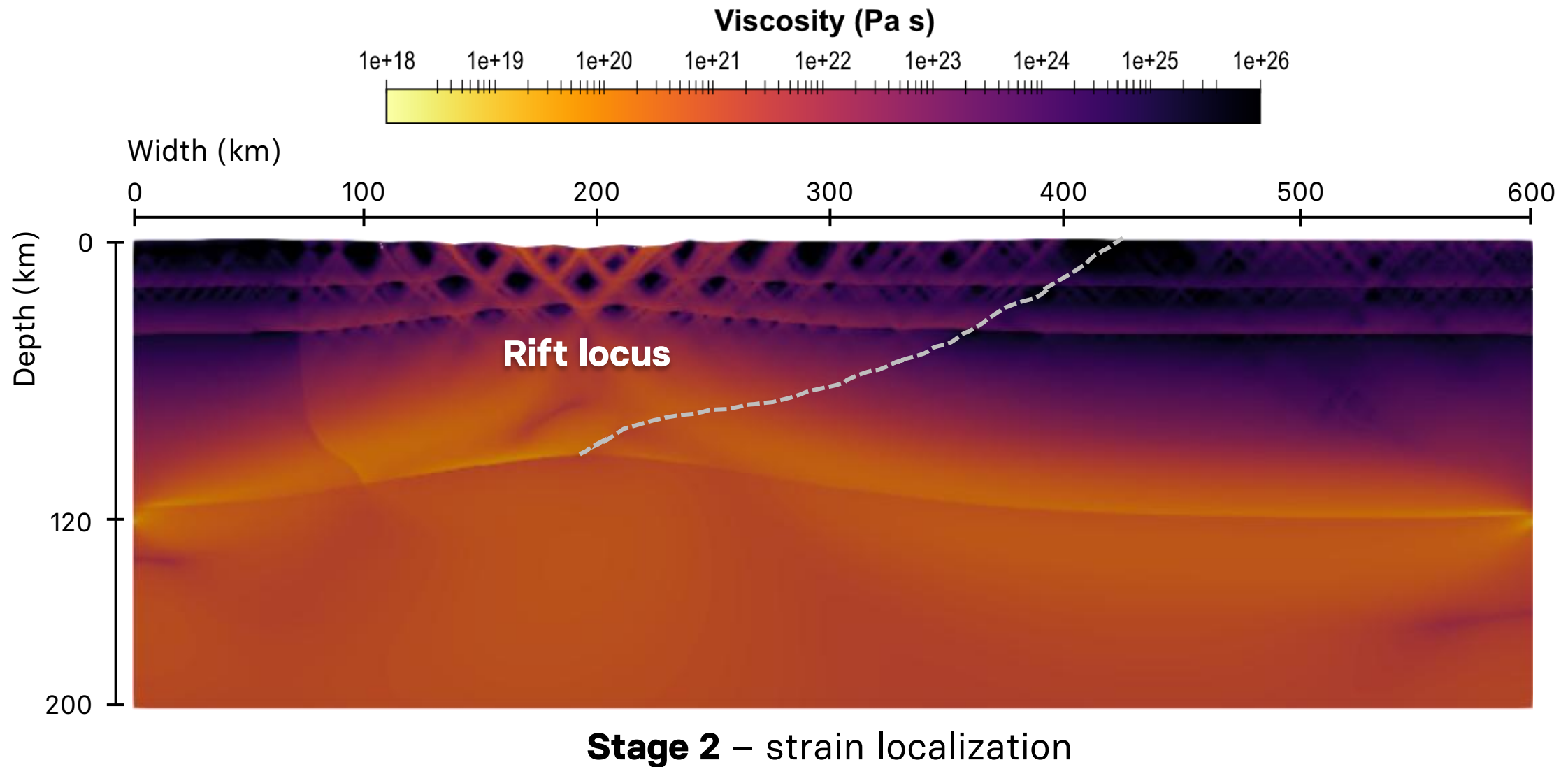
Reference model



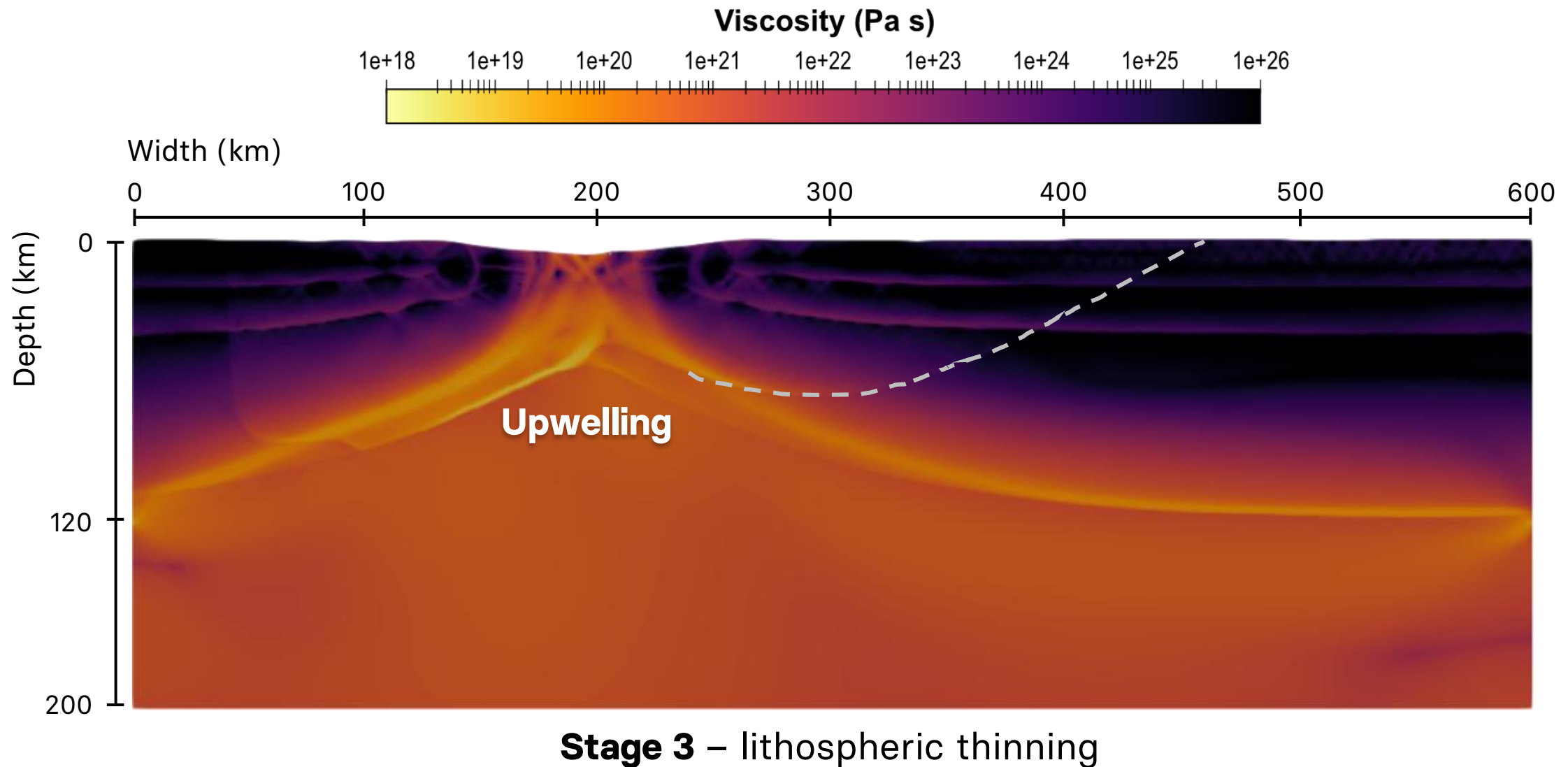
Reference model



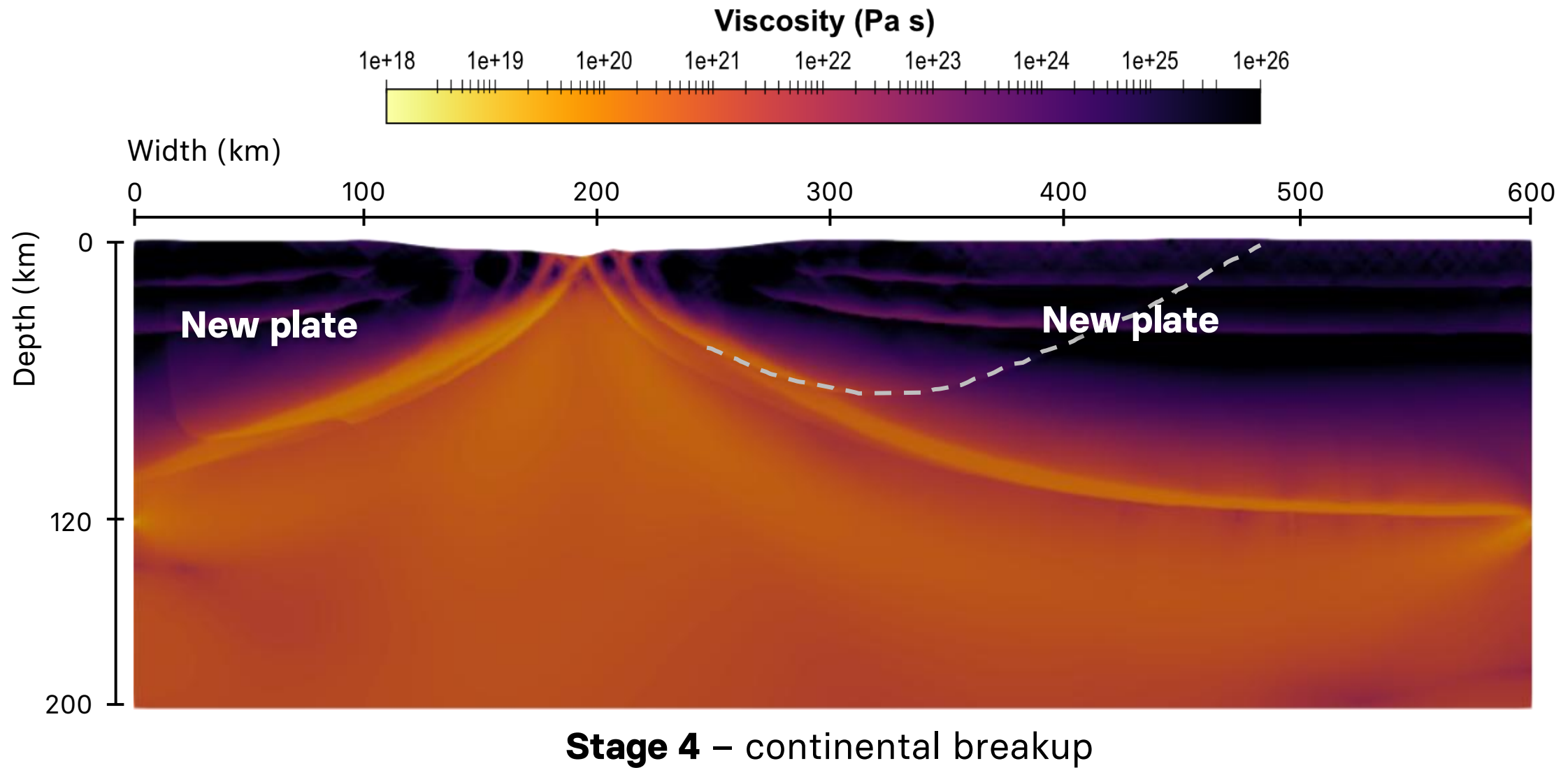
Reference model



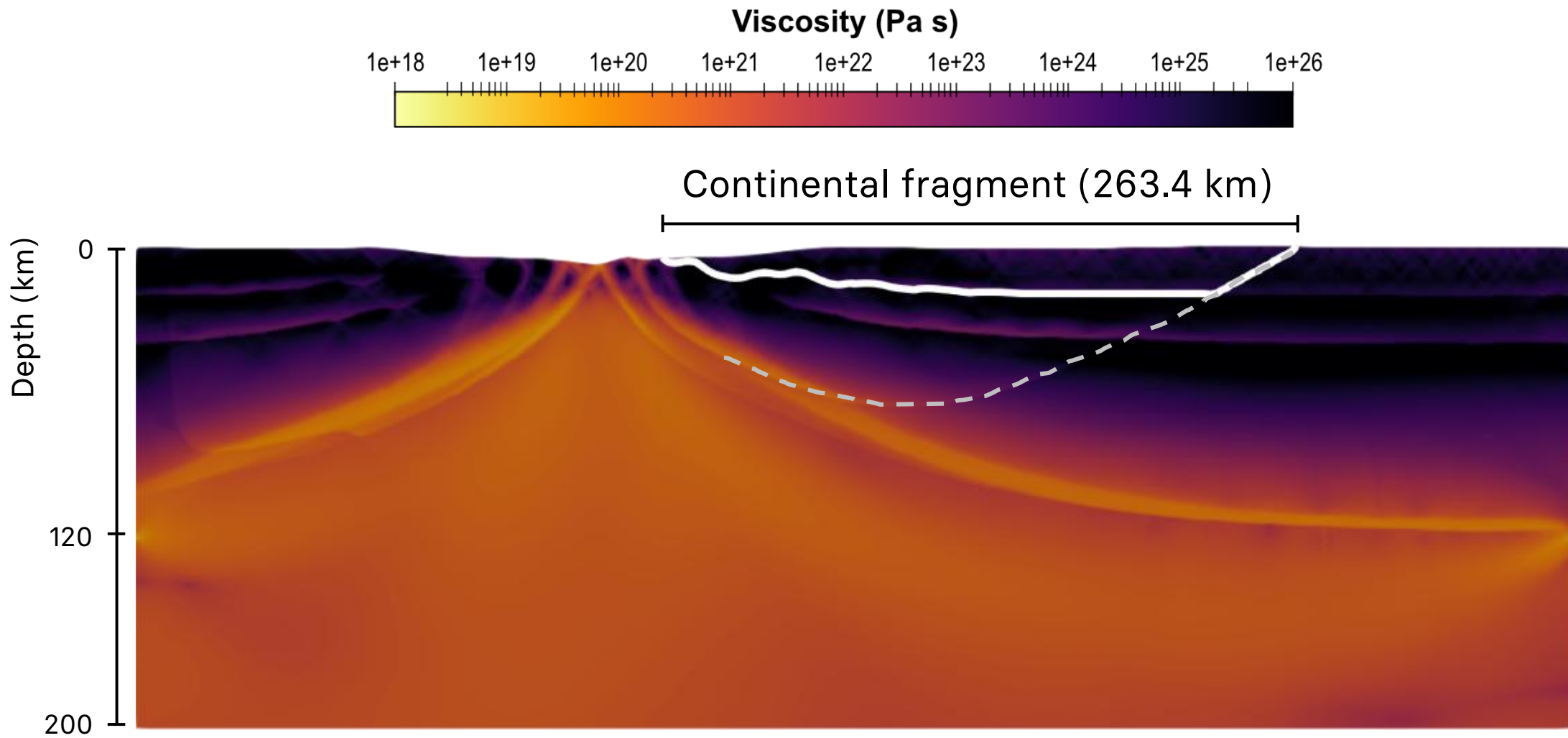
Reference model



Reference model



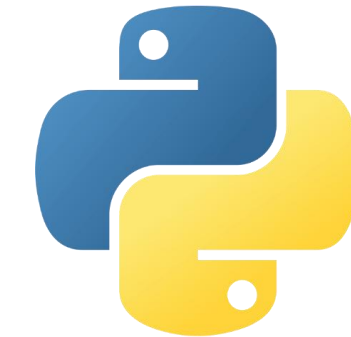
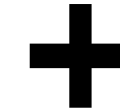
Reference model



Automated data analysis

- From the reference model, we systematically tested **8 physical parameters**, resulting in **94 models** and over **5000 output files**.
- We implemented an **automated system** that sorts through and analyzes all output files.
- This system detects **the time of continental breakup** (i.e., when asthenospheric rocks ascends to the surface) and measures **the width of the continental fragment** (the width of upper crust of the separated continent).

ParaView



Python

Automated data analysis

Model output

solution-00000.0000.vtu

solution-00000.pvtu

solution-00001.0000.vtu

solution-00001.pvtu

solution-00002.0000.vtu

solution-00002.pvtu

solution-00002.0000.ytu

solution-00003.pytut

solution-00003 0000.vtu

solution-00004.pytu

solution_00004_0000.vtu

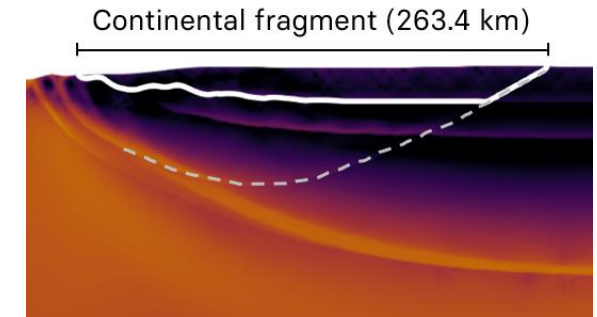
Gerya (2019)

| | | | | | | | | | |
|----------|----------|----------|---------|----------|---|-----|------|----------|---------|
| 0.00E+00 | 9.00E-09 | 0.00E+00 | 1.0E-06 | -2.8E-09 | 0 | 10 | 971 | 1.00E-06 | 3.0E-05 |
| 0.00E+00 | 9.00E-09 | 0.00E+00 | 1.0E-06 | -2.8E-09 | 0 | 41 | 1022 | 1.00E-06 | 3.0E-05 |
| 0.00E+00 | 9.00E-09 | 0.00E+00 | 1.0E-06 | -2.8E-09 | 0 | 103 | 1064 | 1.00E-06 | 3.0E-05 |
| 0.00E+00 | 9.00E-09 | 0.00E+00 | 1.0E-06 | -2.8E-09 | 0 | 154 | 1105 | 1.00E-06 | 3.0E-05 |
| 0.00E+00 | 9.00E-09 | 0.00E+00 | 1.0E-06 | -2.8E-09 | 0 | 185 | 1126 | 1.00E-06 | 3.0E-05 |
| 0.00E+00 | 9.00E-09 | 0.00E+00 | 1.0E-06 | -2.8E-09 | 0 | 194 | 1135 | 1.00E-06 | 3.0E-05 |
| 0.00E+00 | 9.00E-09 | 0.00E+00 | 1.0E-06 | -2.8E-09 | 0 | 198 | 1166 | 1.00E-06 | 3.0E-05 |
| 0.00E+00 | 9.00E-09 | 0.00E+00 | 1.0E-06 | -2.8E-09 | 0 | 219 | 1196 | 1.00E-06 | 3.0E-05 |
| 0.00E+00 | 9.00E-09 | 0.00E+00 | 1.0E-06 | -2.8E-09 | 0 | 229 | 1227 | 1.00E-06 | 3.0E-05 |
| 0.00E+00 | 9.00E-09 | 0.00E+00 | 1.0E-06 | -2.8E-09 | 0 | 239 | 1257 | 1.00E-06 | 3.0E-05 |
| 0.00E+00 | 9.00E-09 | 0.00E+00 | 1.0E-06 | -2.8E-09 | 0 | 243 | 1288 | 1.00E-06 | 3.0E-05 |
| 0.00E+00 | 9.00E-09 | 0.00E+00 | 1.0E-06 | -2.8E-09 | 0 | 244 | 1318 | 1.00E-06 | 3.0E-05 |
| 0.00E+00 | 9.00E-09 | 0.00E+00 | 1.0E-06 | -2.8E-09 | 0 | 475 | 1436 | 1.00E-06 | 3.0E-05 |
| 0.00E+00 | 9.00E-09 | 0.00E+00 | 1.0E-06 | -2.8E-09 | 0 | 537 | 1486 | 1.00E-06 | 3.0E-05 |
| 0.00E+00 | 9.00E-09 | 0.00E+00 | 1.0E-06 | -2.8E-09 | 0 | 565 | 1506 | 1.00E-06 | 3.0E-05 |
| 0.00E+00 | 9.00E-09 | 0.00E+00 | 1.0E-06 | -2.8E-09 | 0 | 593 | 1526 | 1.00E-06 | 3.0E-05 |
| 0.00E+00 | 9.00E-09 | 0.00E+00 | 1.0E-06 | -2.8E-09 | 0 | 621 | 1551 | 1.00E-06 | 3.0E-05 |
| 0.00E+00 | 9.00E-09 | 0.00E+00 | 1.0E-06 | -2.8E-09 | 0 | 651 | 1571 | 1.00E-06 | 3.0E-05 |
| 0.00E+00 | 9.00E-09 | 0.00E+00 | 1.0E-06 | -2.8E-09 | 0 | 679 | 1591 | 1.00E-06 | 3.0E-05 |
| 0.00E+00 | 9.00E-09 | 0.00E+00 | 1.0E-06 | -2.8E-09 | 0 | 692 | 1622 | 1.00E-06 | 3.0E-05 |
| 0.00E+00 | 9.00E-09 | 0.00E+00 | 1.0E-06 | -2.8E-09 | 0 | 710 | 1642 | 1.00E-06 | 3.0E-05 |
| 0.00E+00 | 9.00E-09 | 0.00E+00 | 1.0E-06 | -2.8E-09 | 0 | 741 | 1715 | 1.00E-06 | 3.0E-05 |
| 0.00E+00 | 9.00E-09 | 0.00E+00 | 1.0E-06 | -2.8E-09 | 0 | 785 | 1746 | 1.00E-06 | 3.0E-05 |
| 0.00E+00 | 9.00E-09 | 0.00E+00 | 1.0E-06 | -2.8E-09 | 0 | 813 | 1776 | 1.00E-06 | 3.0E-05 |
| 0.00E+00 | 9.00E-09 | 0.00E+00 | 1.0E-06 | -2.8E-09 | 0 | 847 | 1806 | 1.00E-06 | 3.0E-05 |
| 0.00E+00 | 9.00E-09 | 0.00E+00 | 1.0E-06 | -2.8E-09 | 0 | 879 | 1836 | 1.00E-06 | 3.0E-05 |
| 0.00E+00 | 9.00E-09 | 0.00E+00 | 1.0E-06 | -2.8E-09 | 0 | 909 | 1870 | 1.00E-06 | 3.0E-05 |
| 0.00E+00 | 9.00E-09 | 0.00E+00 | 1.0E-06 | -2.8E-09 | 0 | 940 | 1900 | 1.00E-06 | 3.0E-05 |
| 0.00E+00 | 9.00E-09 | 0.00E+00 | 1.0E-06 | -2.8E-09 | 0 | 101 | 1971 | 1.00E-06 | 3.0E-05 |
| 0.00E+00 | 9.00E-09 | 0.00E+00 | 1.0E-06 | -2.8E-09 | 0 | 41 | 1662 | 1.00E-06 | 3.0E-05 |
| 0.00E+00 | 9.00E-09 | 0.00E+00 | 1.0E-06 | -2.8E-09 | 0 | 103 | 1684 | 1.00E-06 | 3.0E-05 |
| 0.00E+00 | 9.00E-09 | 0.00E+00 | 1.0E-06 | -2.8E-09 | 0 | 143 | 1704 | 1.00E-06 | 3.0E-05 |
| 0.00E+00 | 9.00E-09 | 0.00E+00 | 1.0E-06 | -2.8E-09 | 0 | 128 | 1728 | 1.00E-06 | 3.0E-05 |

~~Unsens~~



Visualize output and
record analytical
procedures in
Python.



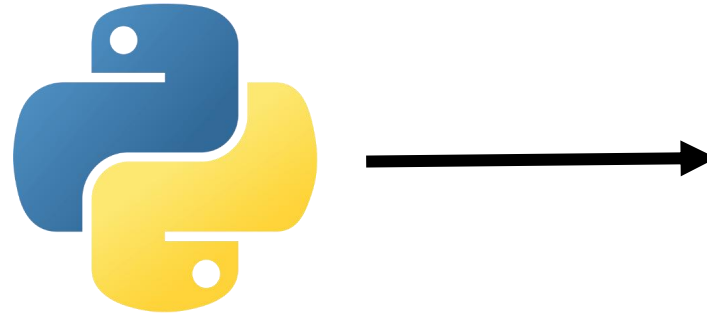
Quantify ASPECT
model observation
(e.g., continental
fragment width)

Automated data analysis

Model output

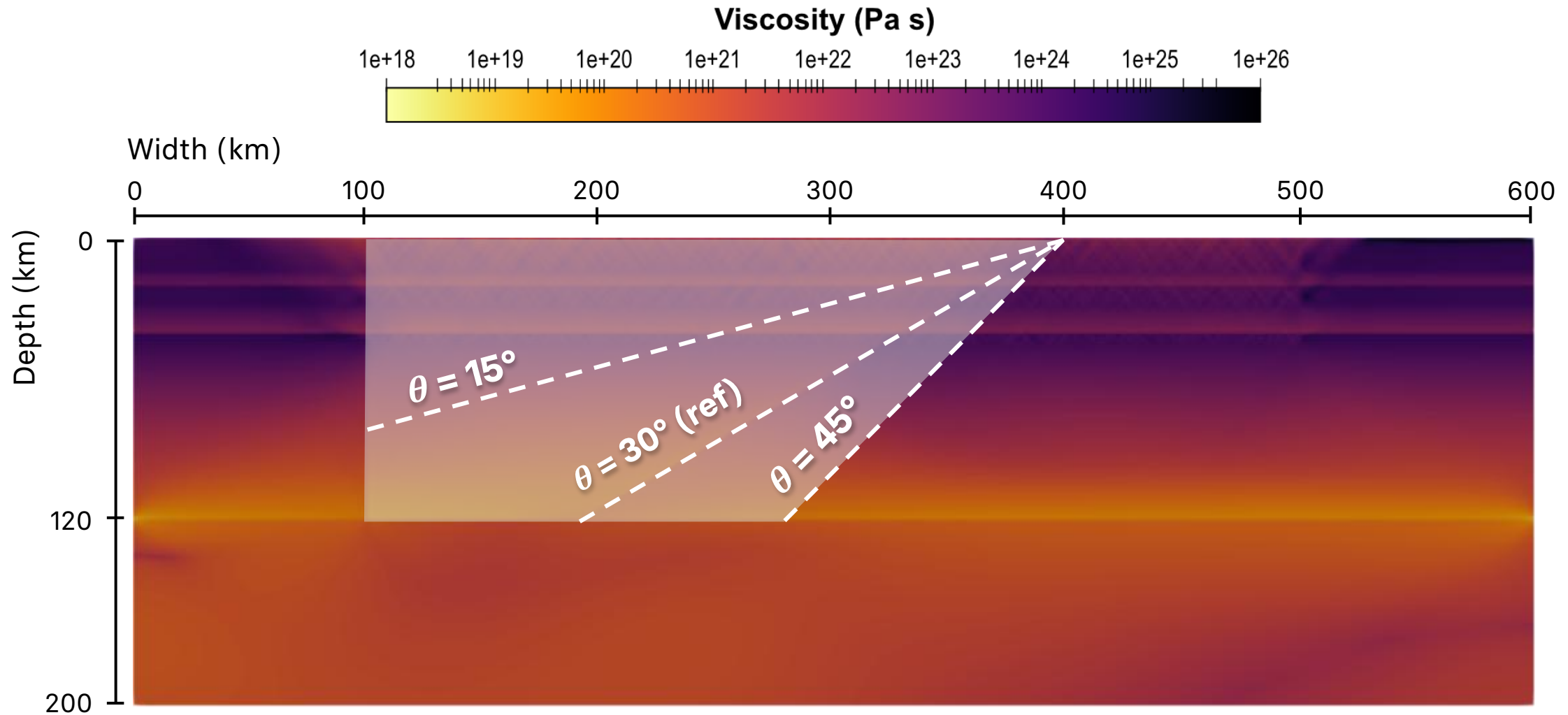
solution-00000.0000.vtu
solution-00000.pvtu
solution-00001.0000.vtu
solution-00001.pvtu
solution-00002.0000.vtu
solution-00002.pvtu
solution-00002.0000.vtu
solution-00003.pvtu
solution-00003.0000.vtu
solution-00004.pvtu
solution-00004.0000.vtu
...

The power of
for loops



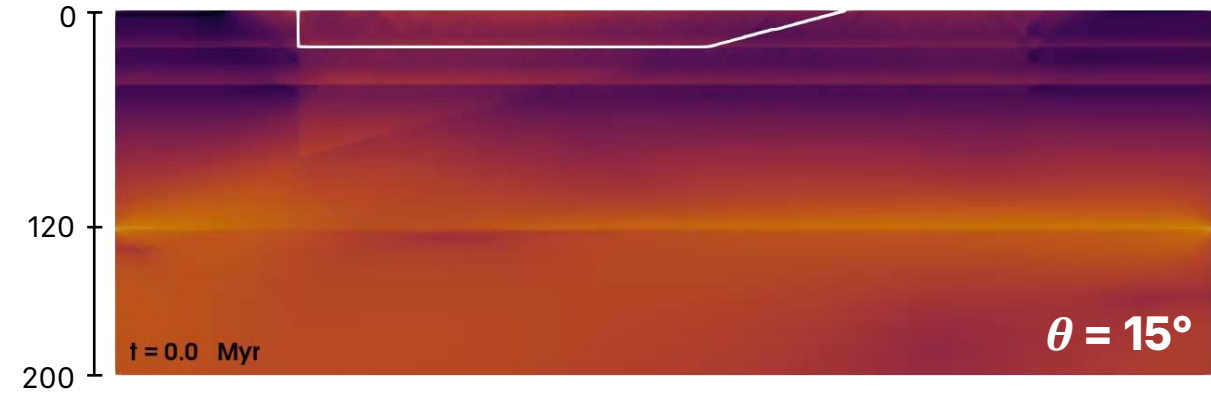
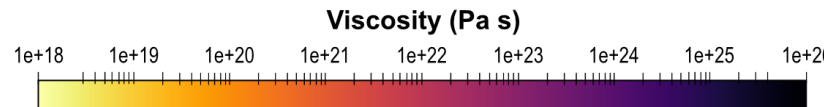
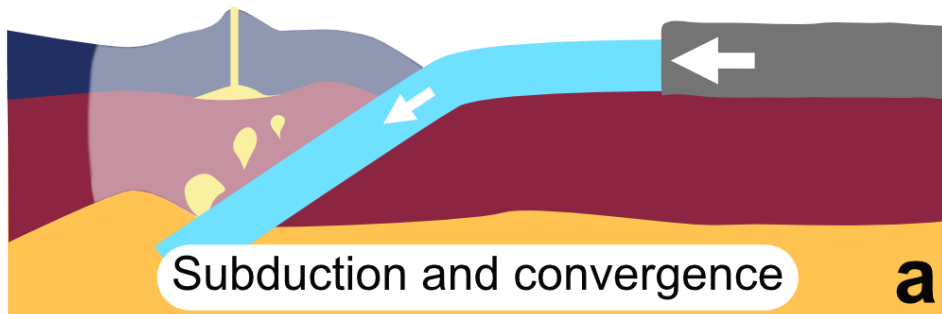
Over 90% reduction in
time of analysis vs
manual measurements.
Consistent results.

Dip angle of old suture



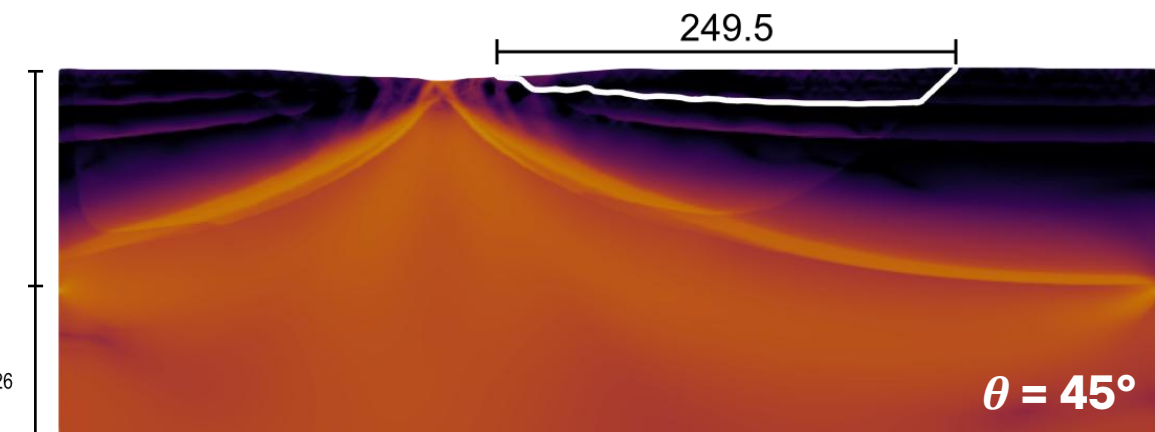
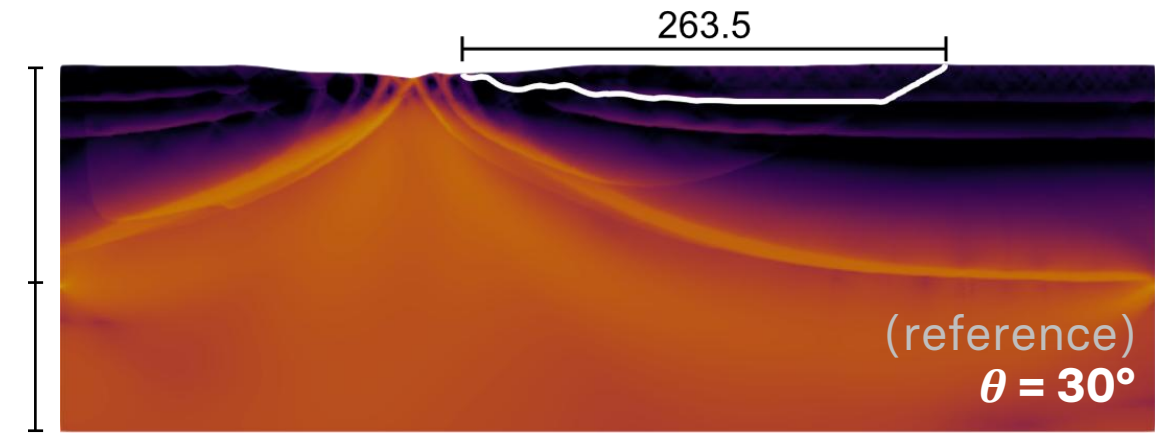
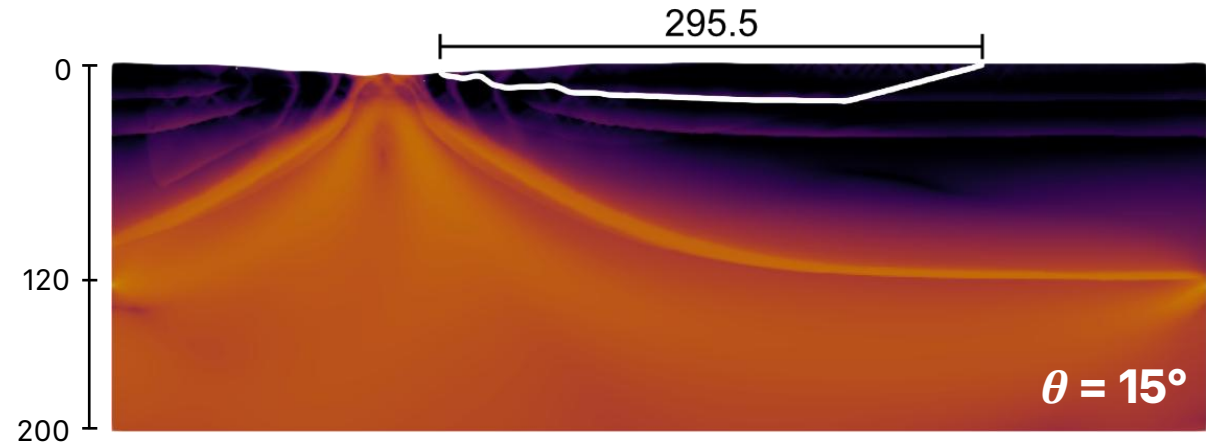
Dip angle of old suture

Geometry of subduction-related rheological weakness



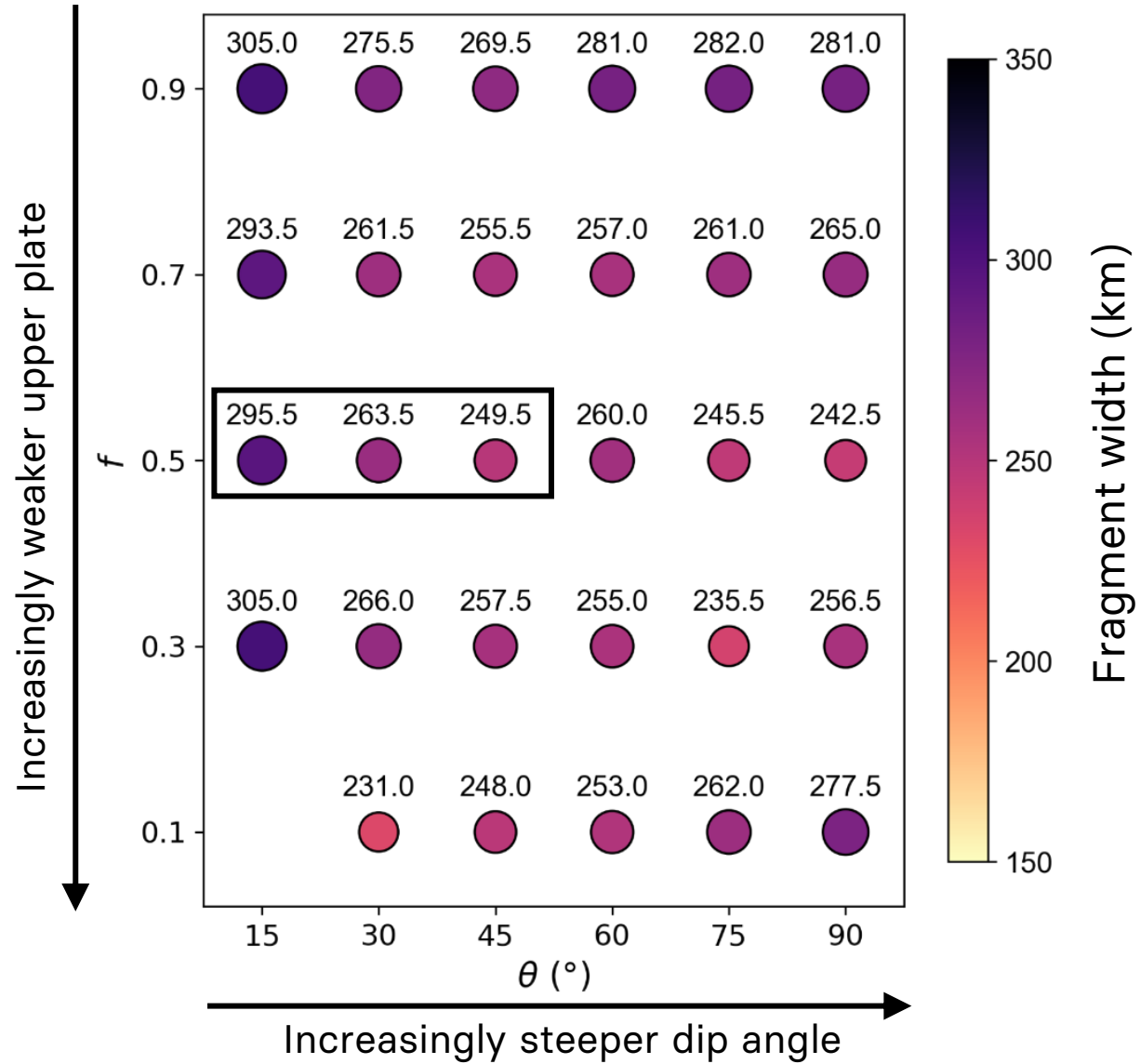
Dip angle of old suture

- $\theta = 15^\circ - 45^\circ$: a **steeper** dip angle creates a **smaller** fragment

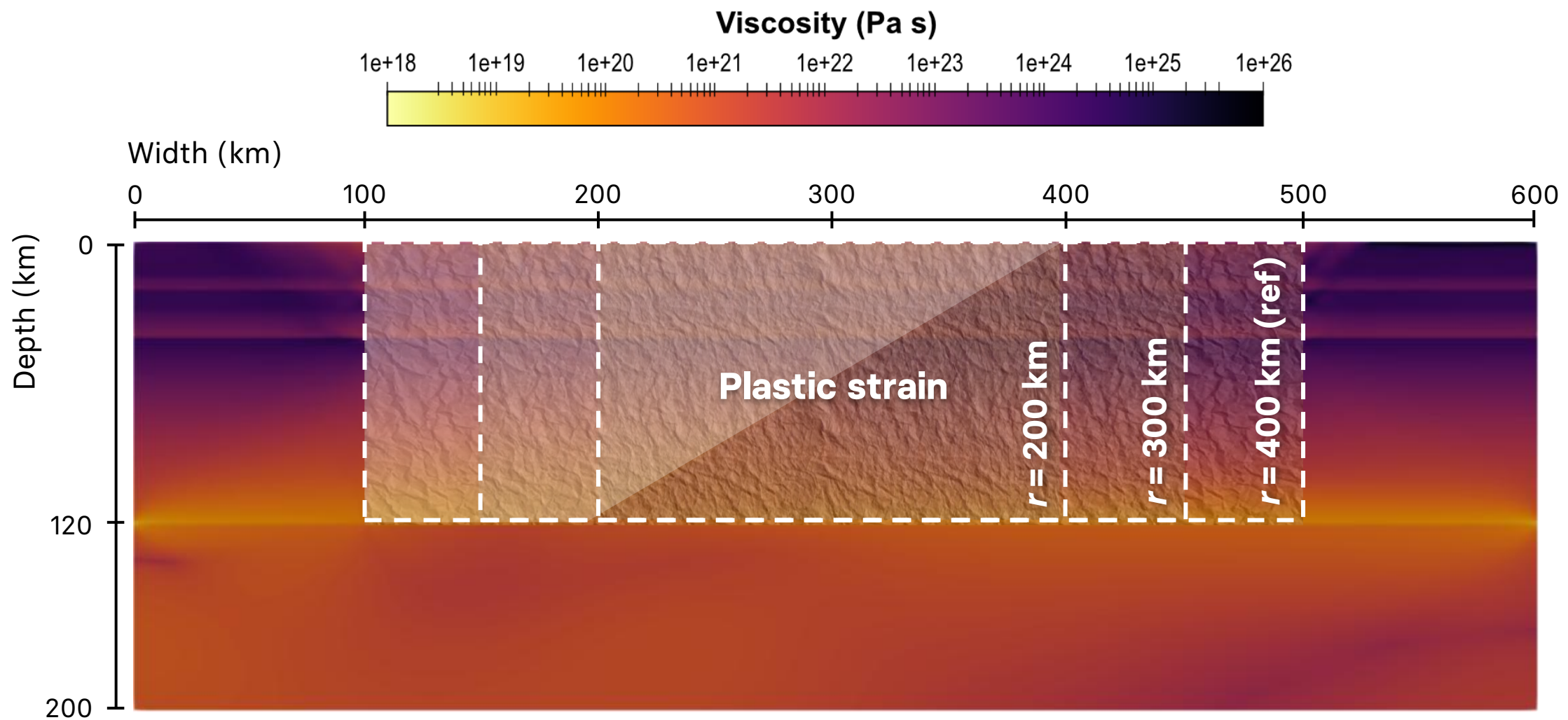


Dip angle of old suture

- $\vartheta = 15^\circ - 45^\circ$: a **steeper** dip angle creates a **smaller** fragment
- $\vartheta = 60^\circ - 90^\circ$: more **random** variations in fragment widths
- $f = 0.1$: a steeper dip angle, however, creates a larger fragment.



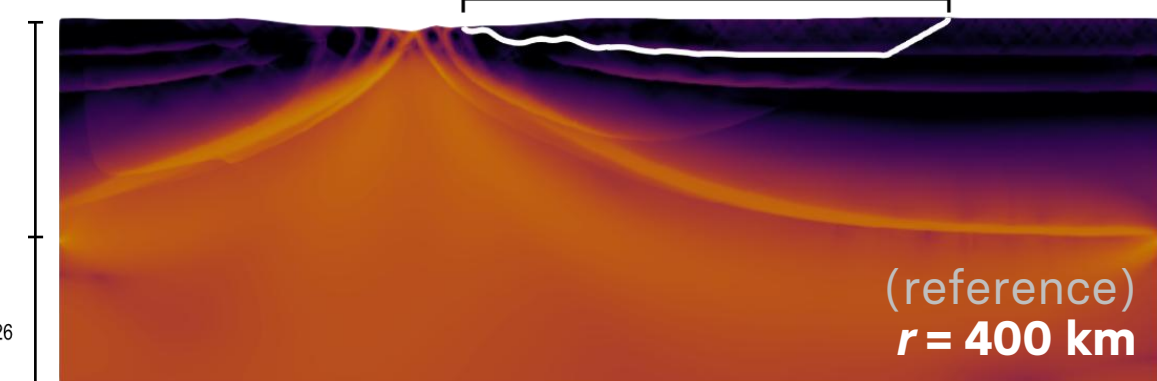
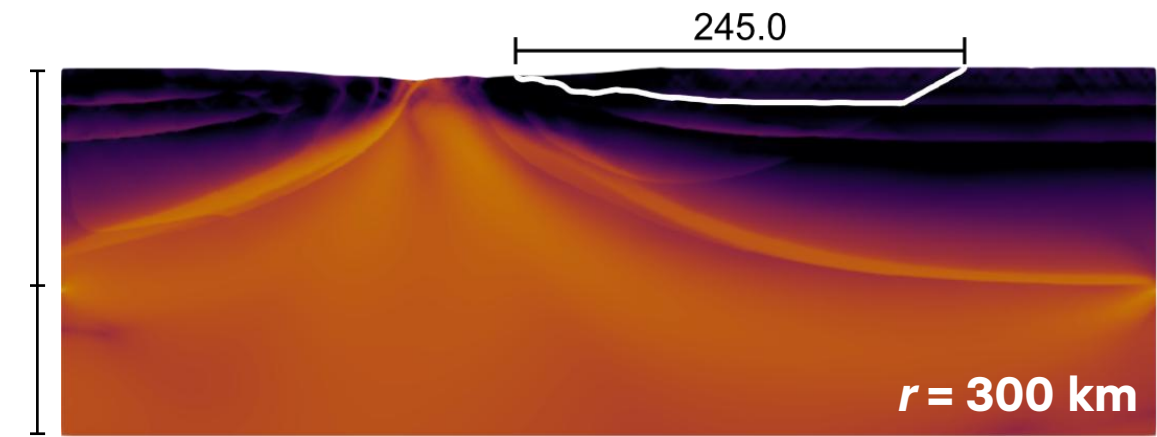
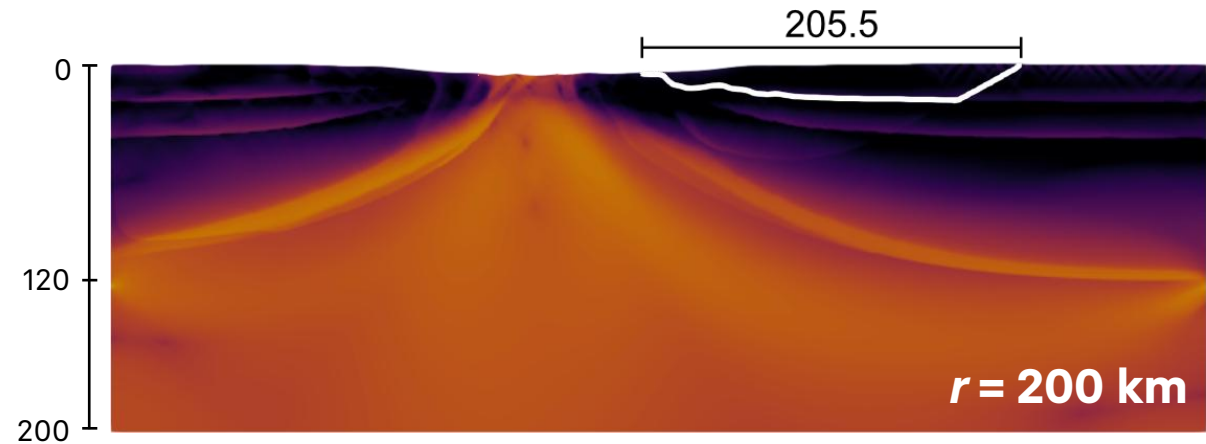
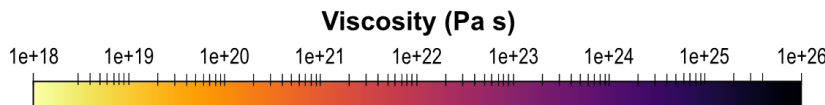
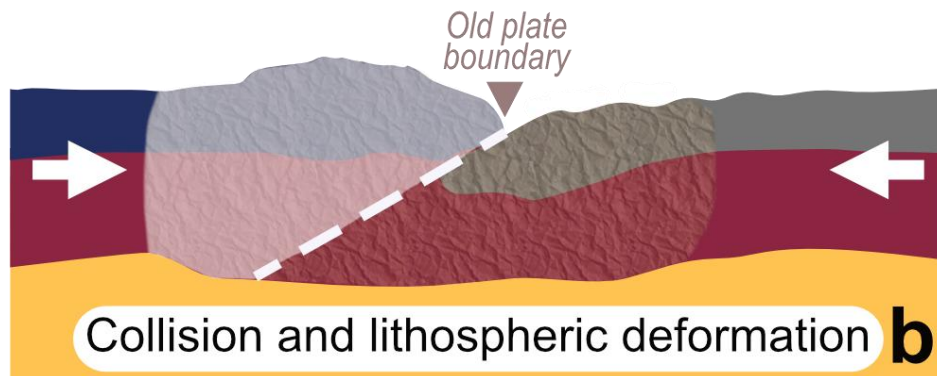
Extent of orogenic deformation



Extent of orogeny

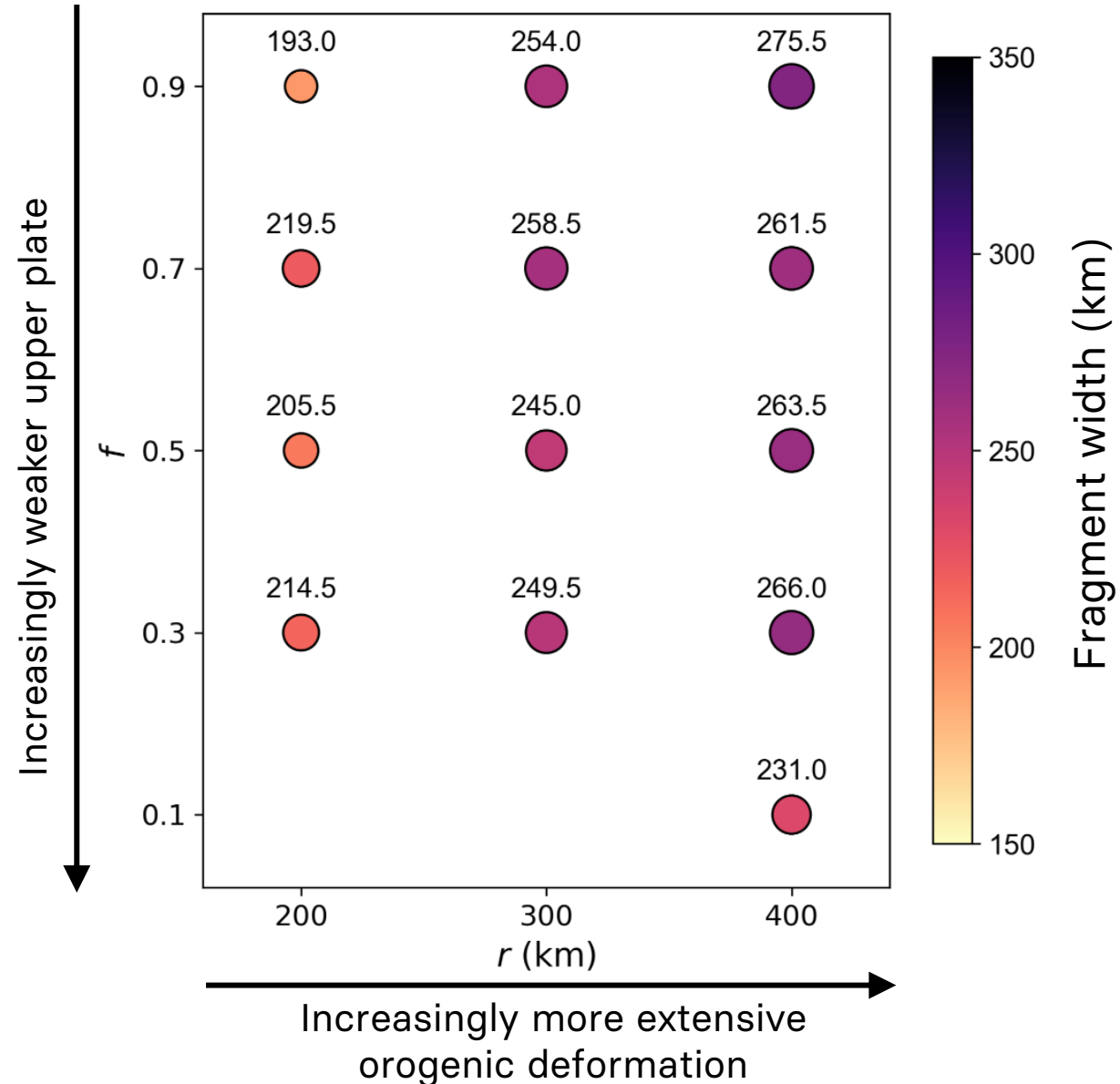
- A **more extensive** deformation zone creates a **larger** fragment.

Geometry of orogenesis-related strain weakness

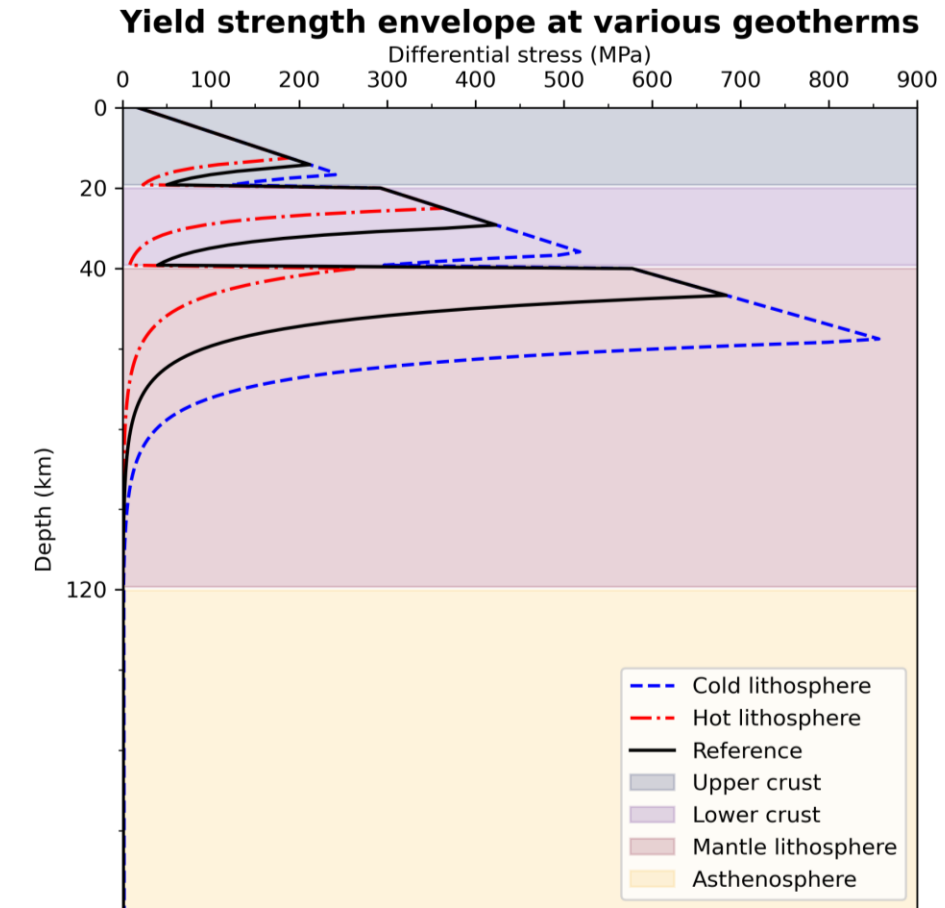
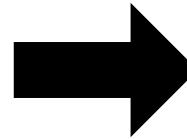
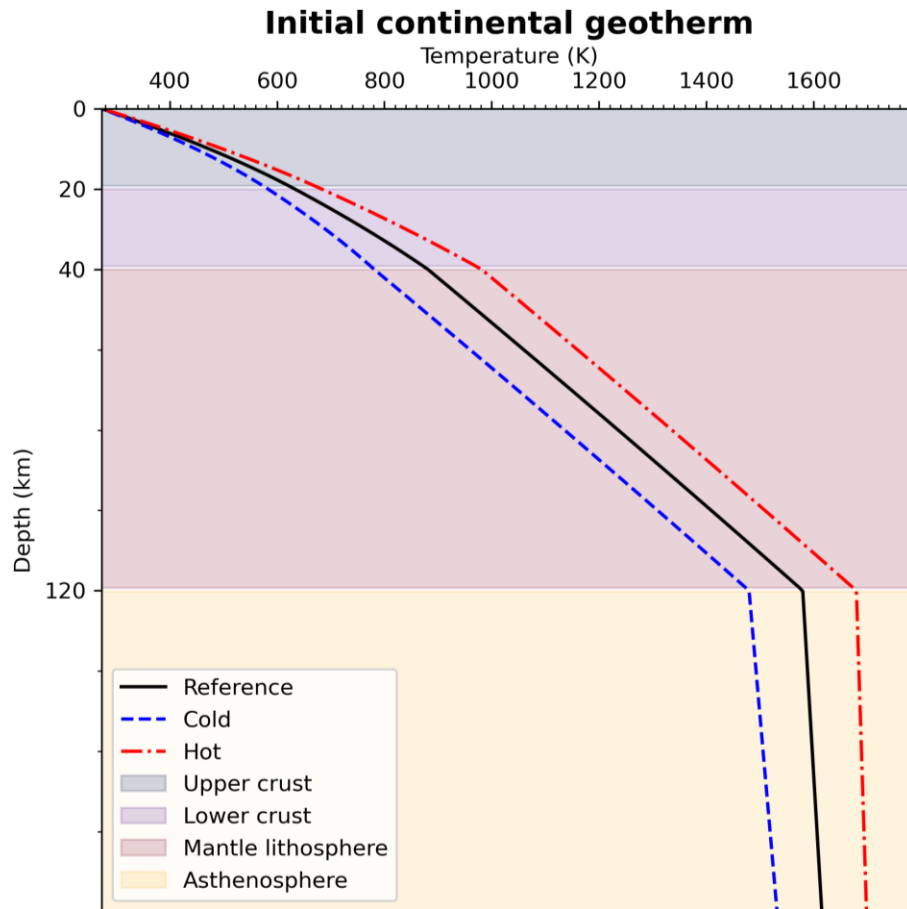


Extent of orogeny

- **More extensive** orogenic deformation creates a **larger** fragment.
- $f = 0.1$: some models fail due to the nonlinearity of ductile deformation.

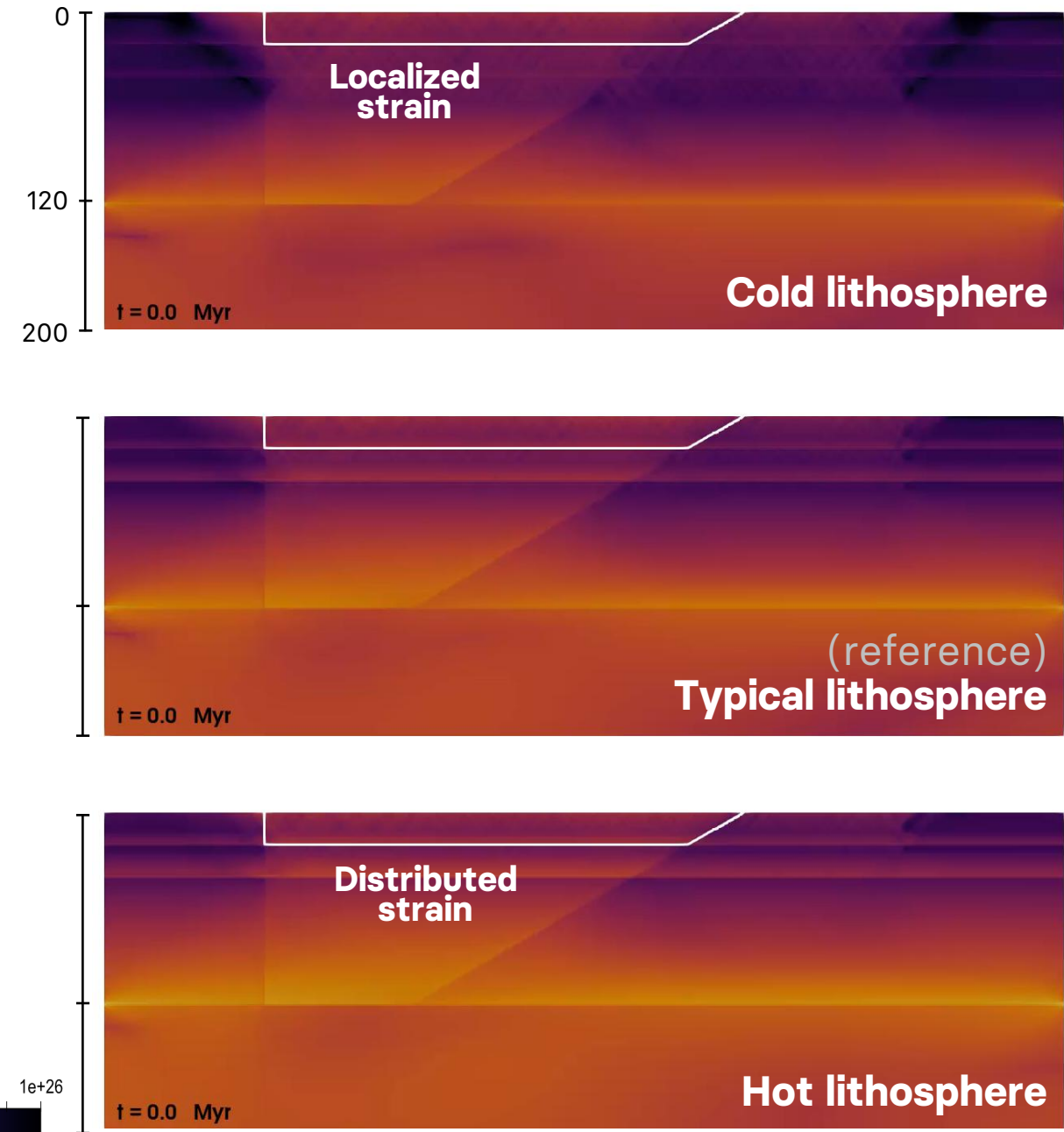
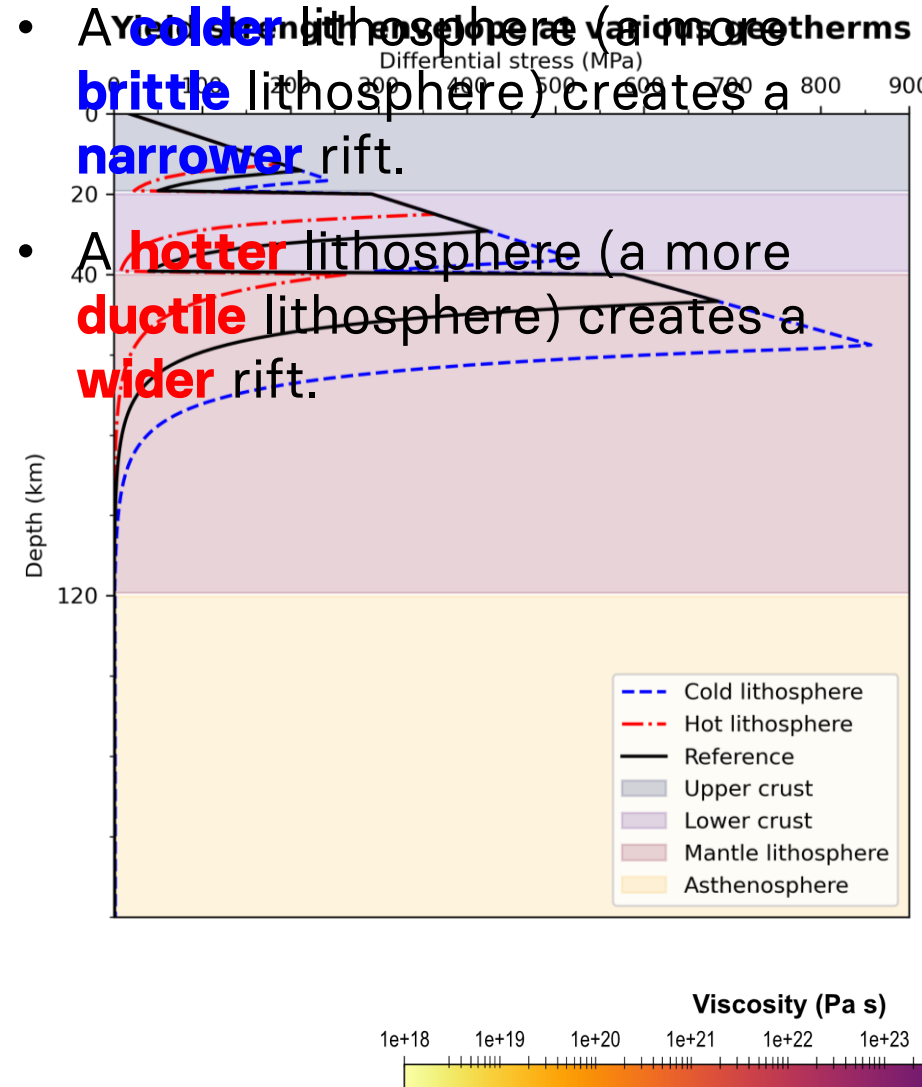


Initial model geotherm



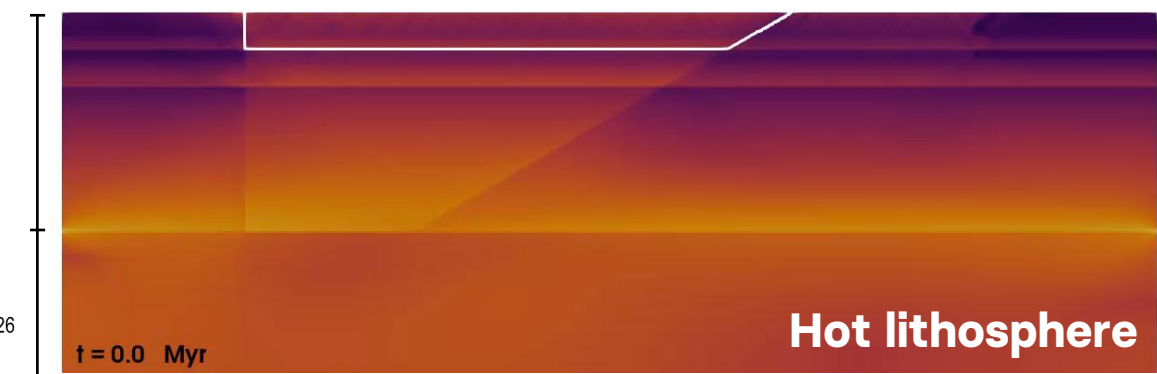
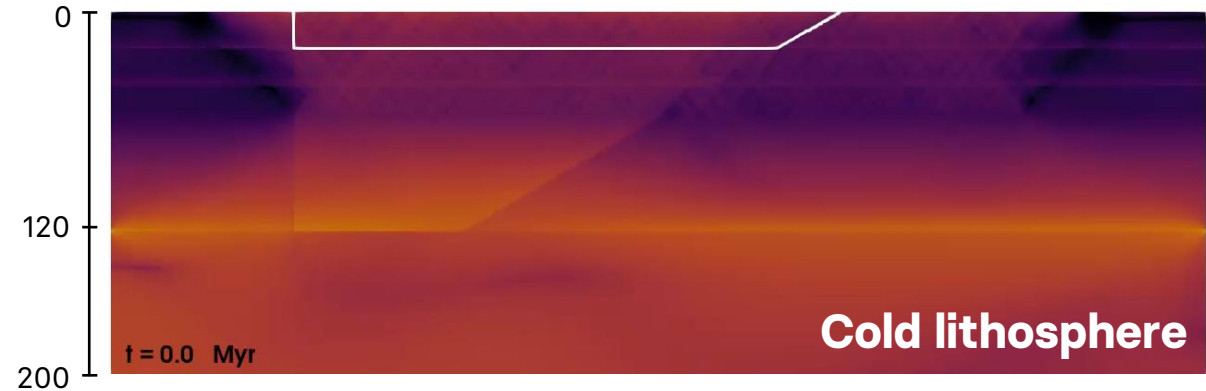
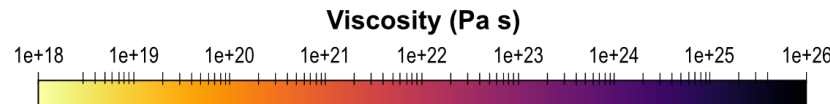
- A **colder** geotherm leads to a more **brittle** lithosphere.
- A **hotter** geotherm leads to a more **ductile** lithosphere.

Initial model geotherm



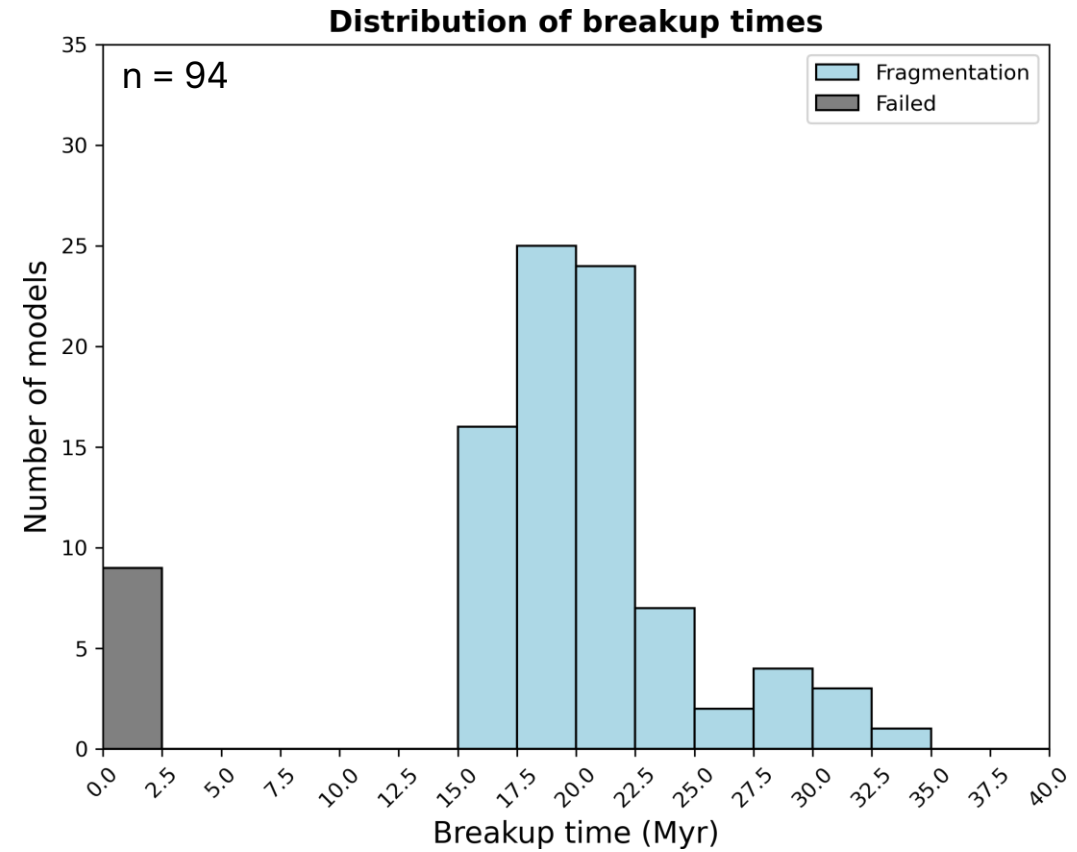
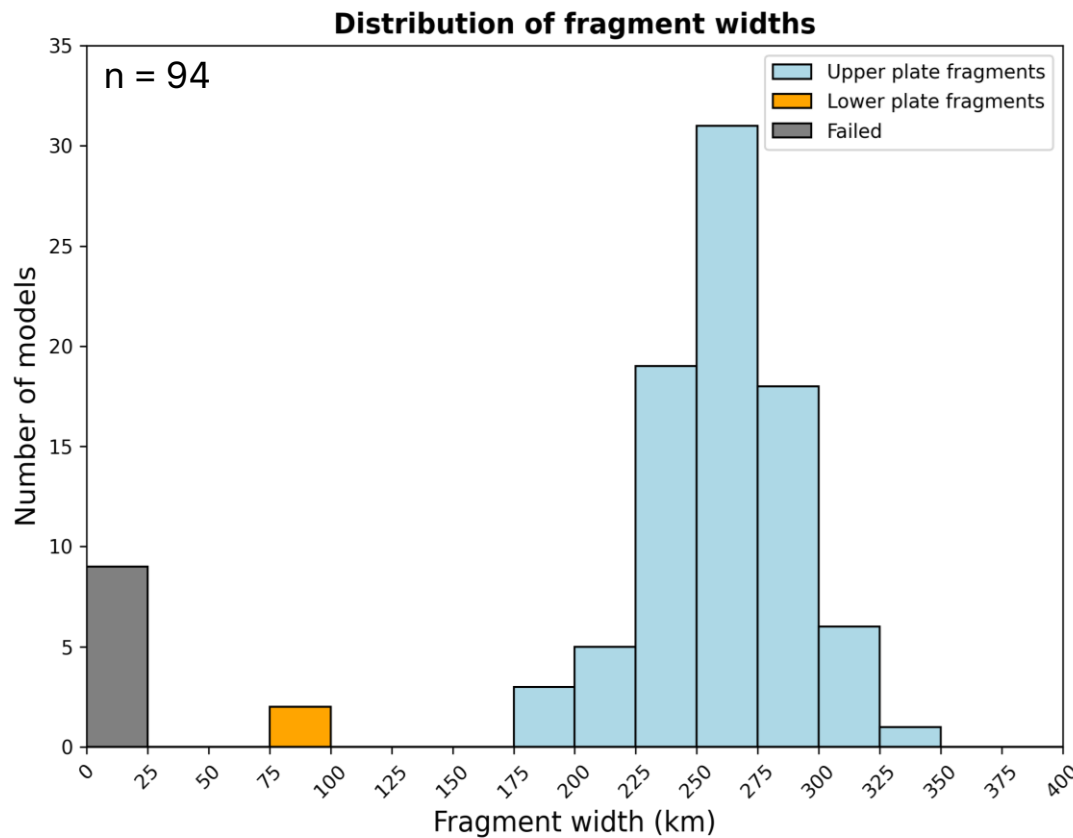
Initial model geotherm

- A **colder** lithosphere (a more **brittle** lithosphere) creates a **narrower** rift.
- A **hotter** lithosphere (a more **ductile** lithosphere) creates a **wider** rift.
- The initial geotherm influences **strain localization** during rifting.



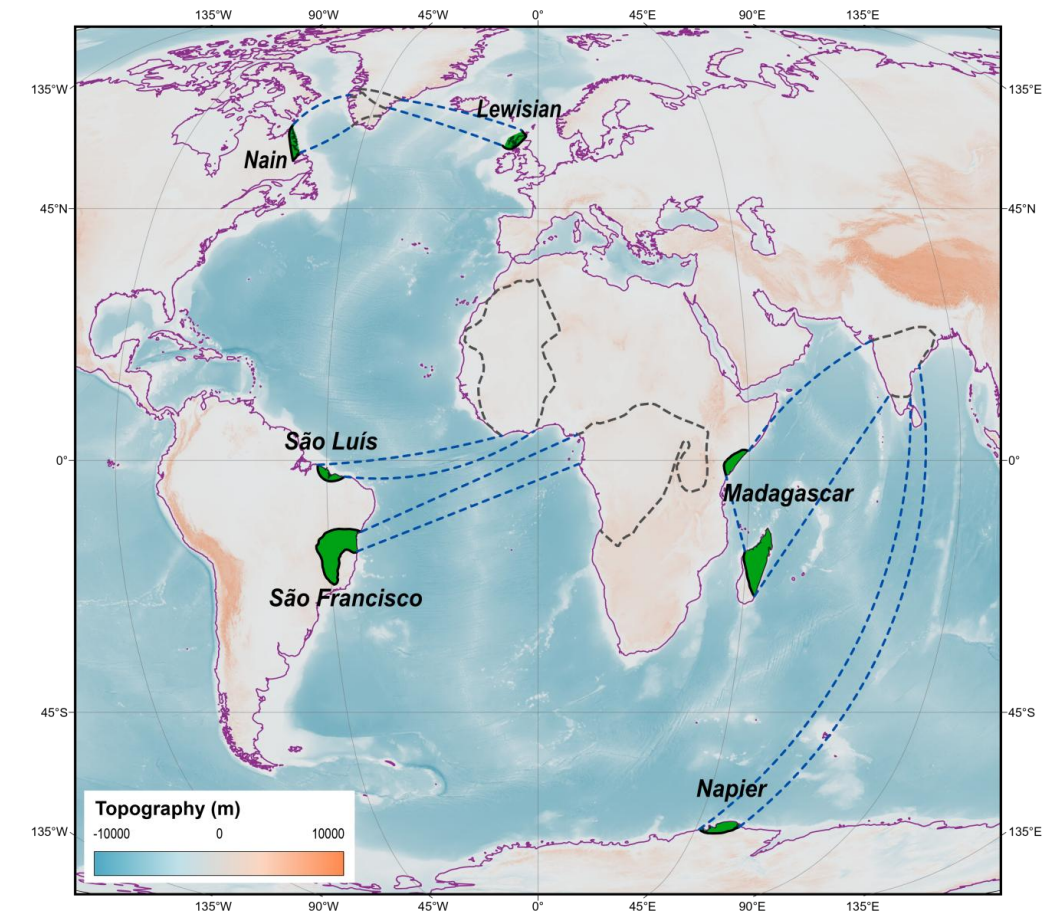
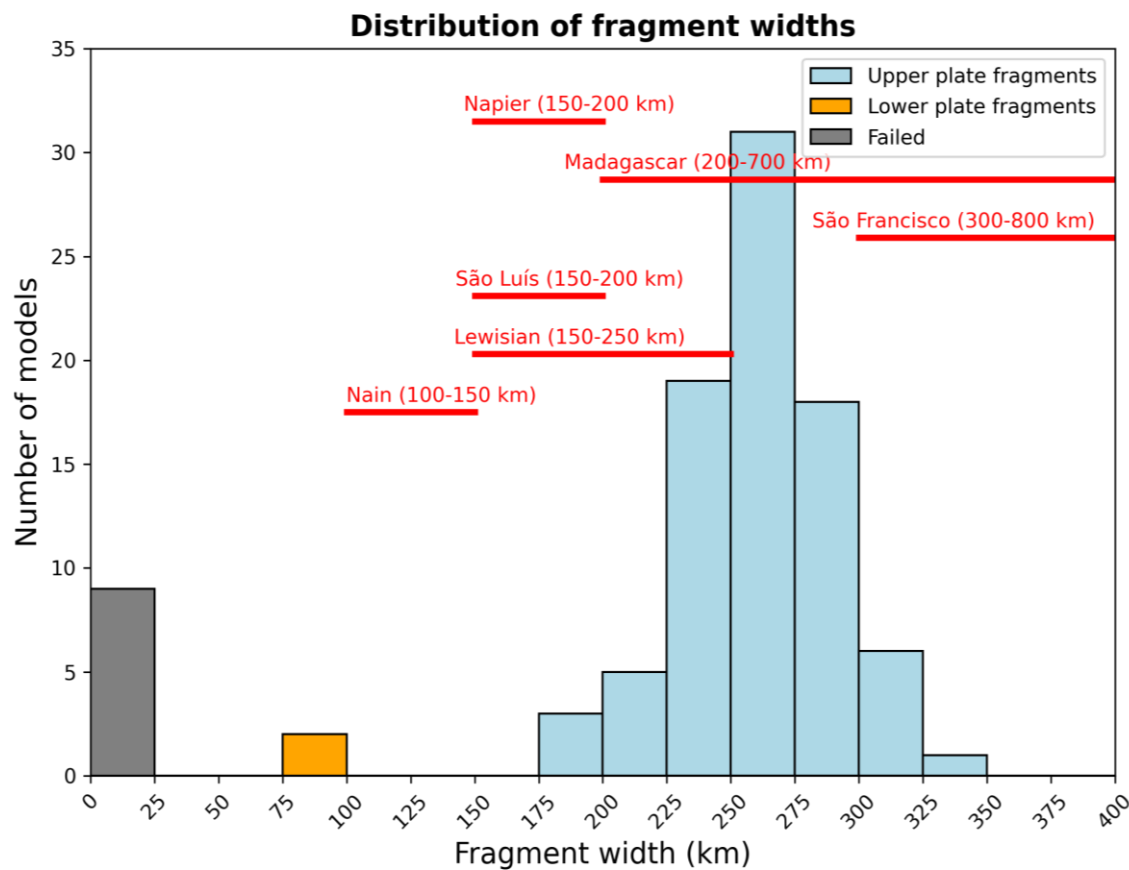
Model summary

- We produce fragments in widths of **~175–350 km** over **~15–35 Myr.**



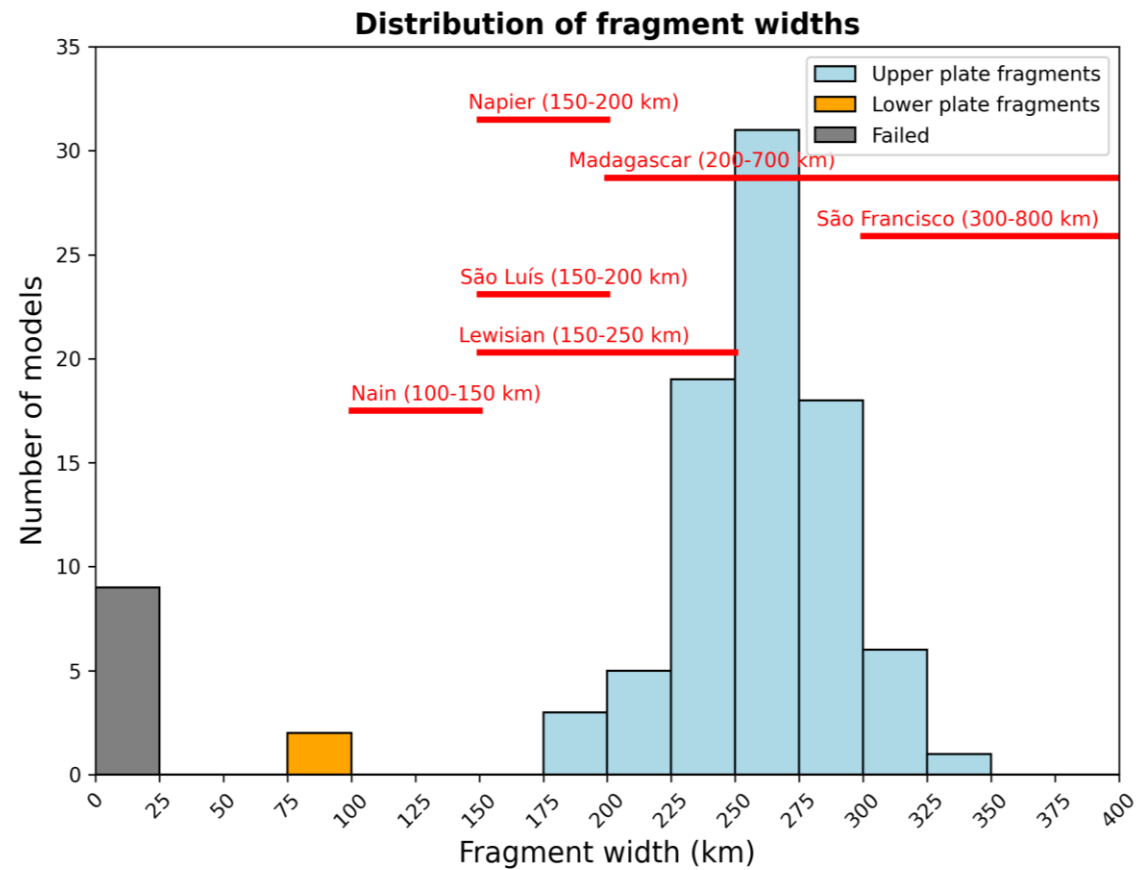
Comparison with geological examples

- Our modelled fragment widths align with many geological examples.
 - All examples above experienced **several episodes of Wilson Cycles**.



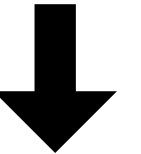
Conclusions

- Using an automated system, we quantify the **influence of structural inheritance** in fragment formation.
- The **geometry of inherited structures** directly controls the fragment width.
- However, the rift process can also be influenced by the **initial geotherm** (and other factors).
- Our modelled fragments **align with many geological examples**.
- We provide a **tectonic recipe** for future regional models.



Thank you!

Access to setup, tutorial, code, and data



github.com/alanjyu/fragment_recipe



Governing equations

$$\nabla \cdot \mathbf{u} = 0$$

Mass

$$-\nabla \cdot \mu \dot{\varepsilon}(\mathbf{u}) + \nabla P = \rho \mathbf{g}$$

Linear momentum

$$\rho C_p \left(\frac{\partial T}{\partial t} + \mathbf{u} \cdot \nabla T \right) - \nabla \cdot k \nabla T = \rho H$$

Energy

$$\rho = \rho_0 (1 - \alpha (T' - T_0'))$$

Equation of state

Boussinesq approximation

- The compressional Navier-Stokes equations are highly nonlinear and unstable.
- $\frac{\Delta\rho}{\rho} \ll 1$, density variation not considered except in the buoyancy term ρg
- Density is loosely related to temperature.

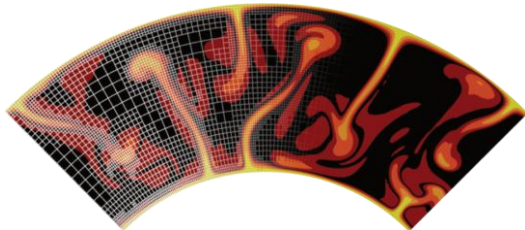
$$\rho = \rho_0(1 - \alpha(T' - T_0'))$$

where $\alpha = -\frac{1}{\rho_0} \left(\frac{\partial \rho}{\partial T}\right)_P$ is the thermal expansivity.

Infinite Prandtl Number

- $Pr = \frac{\text{momentum diffusivity}}{\text{thermal diffusivity}} \sim 10^{25}$ for Earth's mantle
- In physical terms, infinite Pr means that heat conduction is very slow compared to momentum diffusion.

Numerical modelling



ASPECT



Initial physical model

Forward model (in time)

Model output

$$\nabla \cdot \mathbf{u} = 0$$

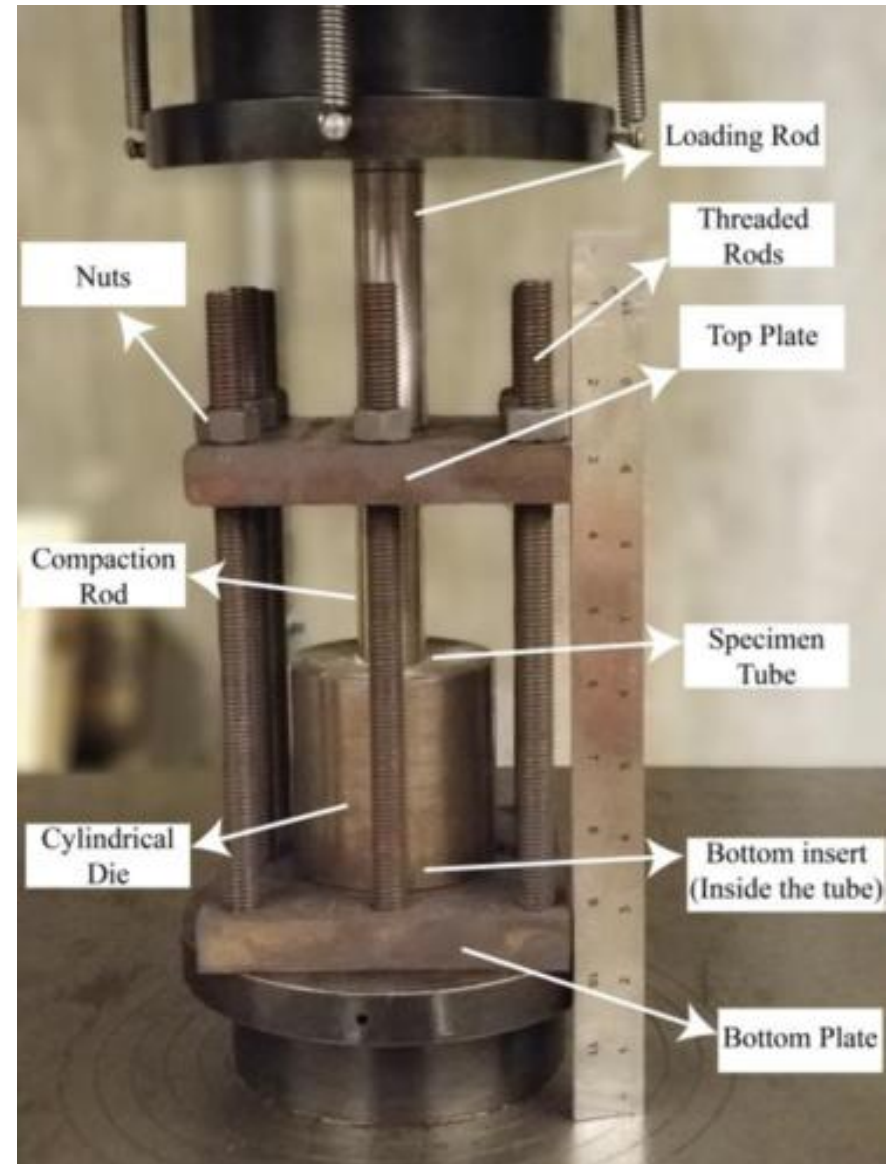
$$-\nabla \cdot \mu \dot{\varepsilon}(\mathbf{u}) + \nabla P = \rho \mathbf{g}$$

$$\rho C_p \left(\frac{\partial T}{\partial t} + \mathbf{u} \cdot \nabla T \right) - \nabla \cdot k \nabla T = \rho H$$

$$\rho = \rho_0 (1 - \alpha (T' - T_0'))$$

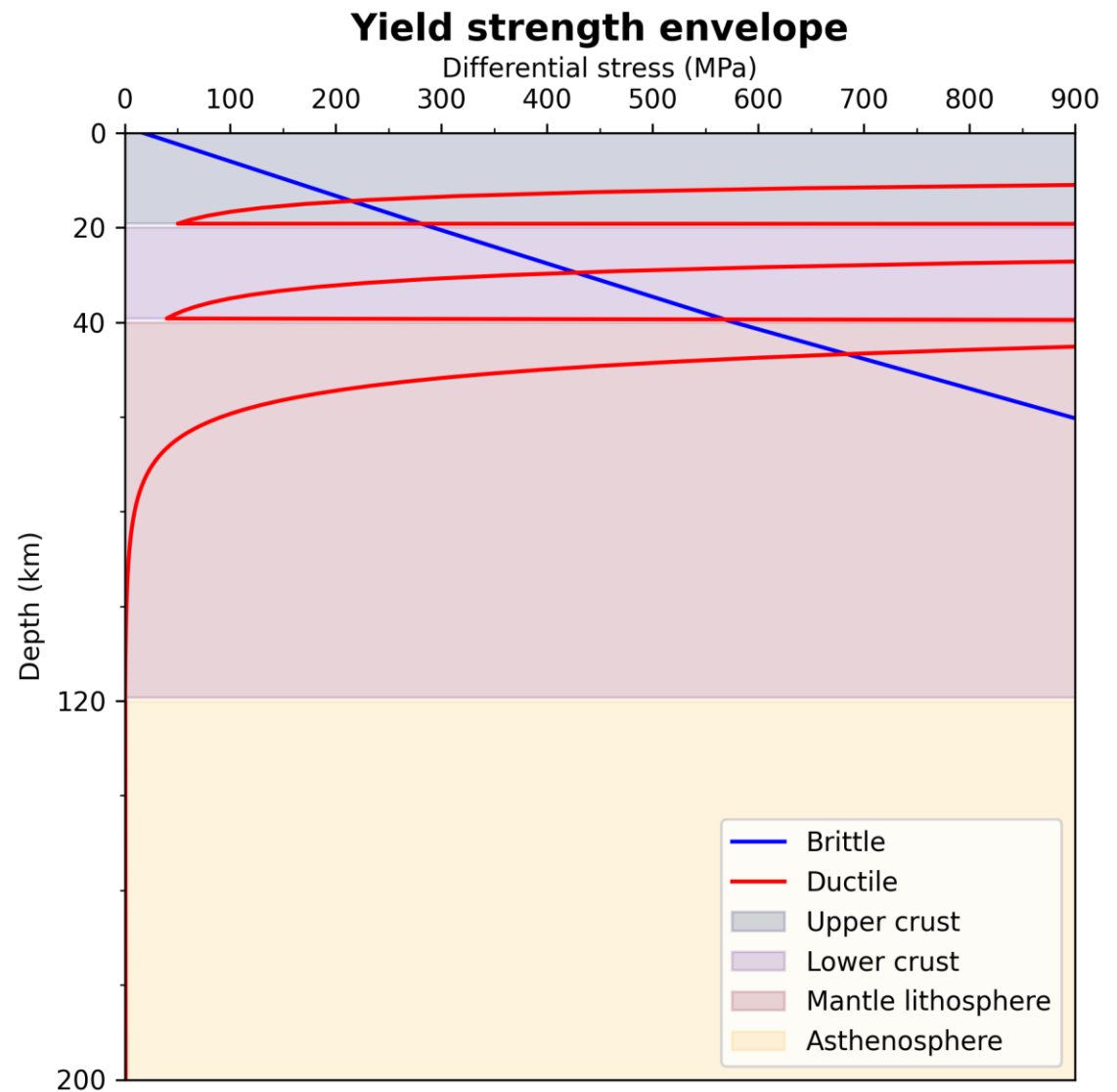
Rheology and flow laws

- Rheology describes the deformation of material.
- Most rocks are **brittle** at room temperature and atmosphere.
- However, they transition to a **ductile** state under mantle-like pressure and temperature.
- The ductile strength of rocks are measured in laboratory experiments (i.e., **flow laws**).
- Here we model both dislocation creep and diffusion creep.



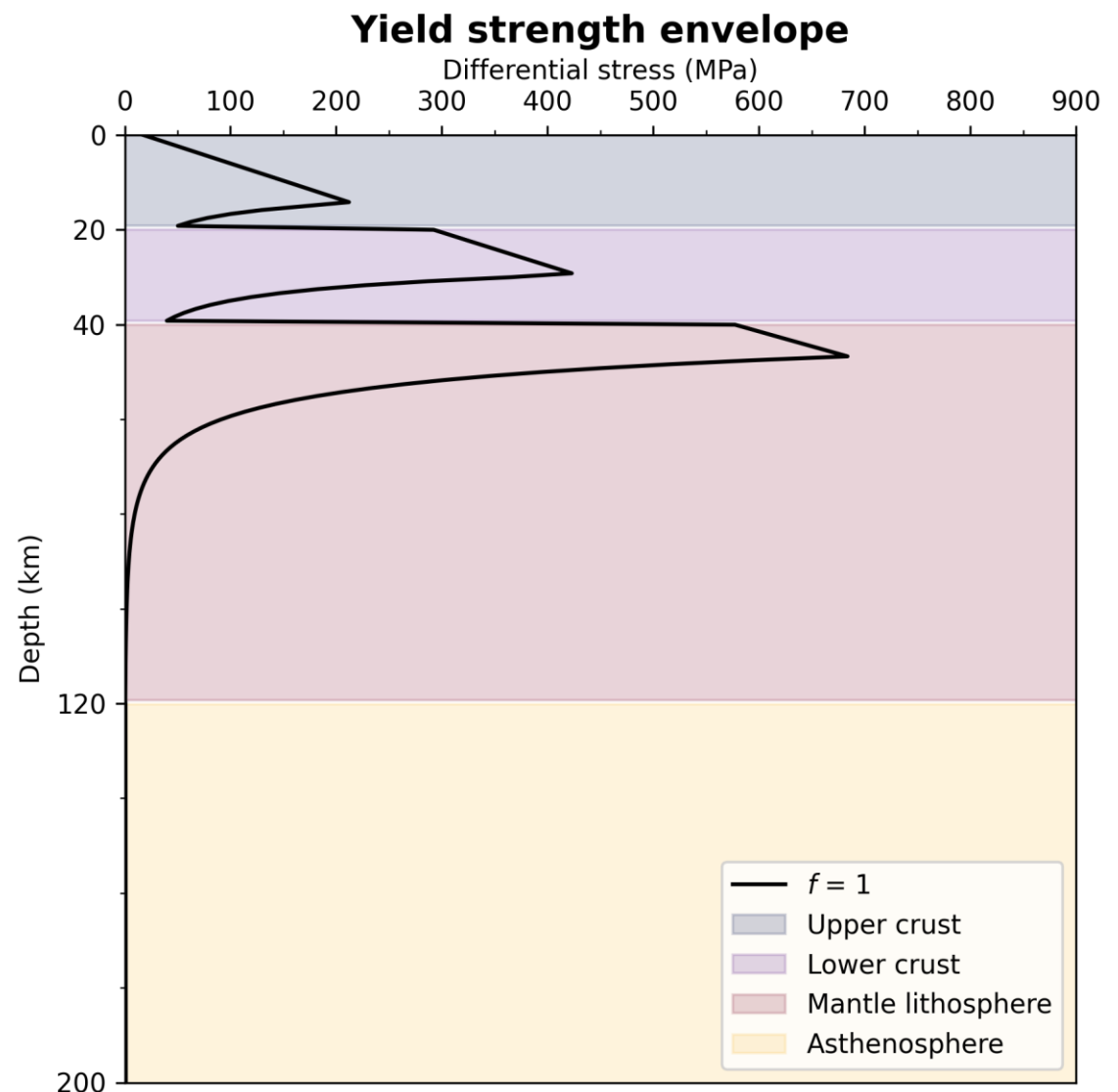
Rheology and flow laws

- ASPECT can simulate both **brittle** and **ductile** deformation.



Rheology and flow laws

- ASPECT can simulate both **brittle** and **ductile** deformation.
- The lithospheric yield strength is determined by the **minimum differential stress** required to deform the rock.

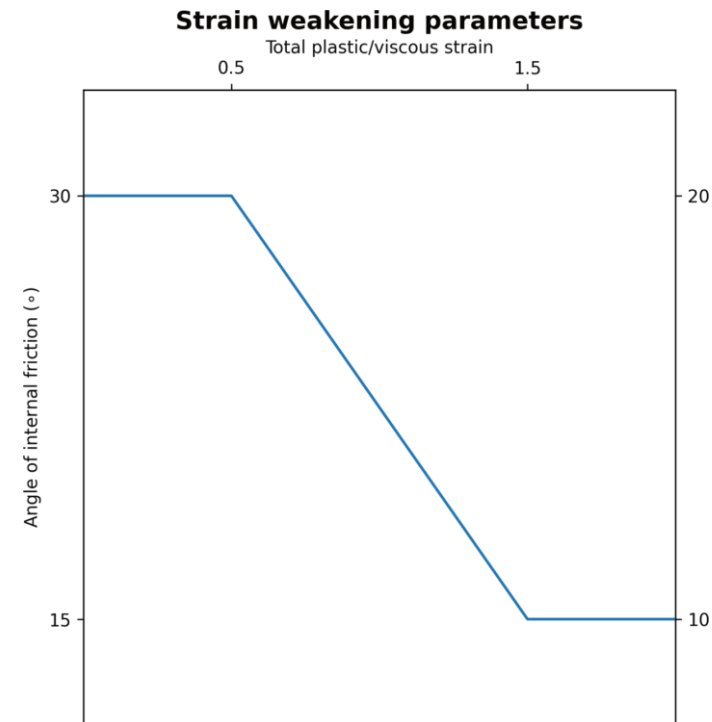


Implementation of structural inheritance

- We use two mechanisms to create structural and rheological heterogeneities.
 - **Strain:** randomly-distributed brittle deformation (to represent varying orogenic deformation)
 - **Rheology:** lower rock strength through viscosity (to represent subduction-related deformation)

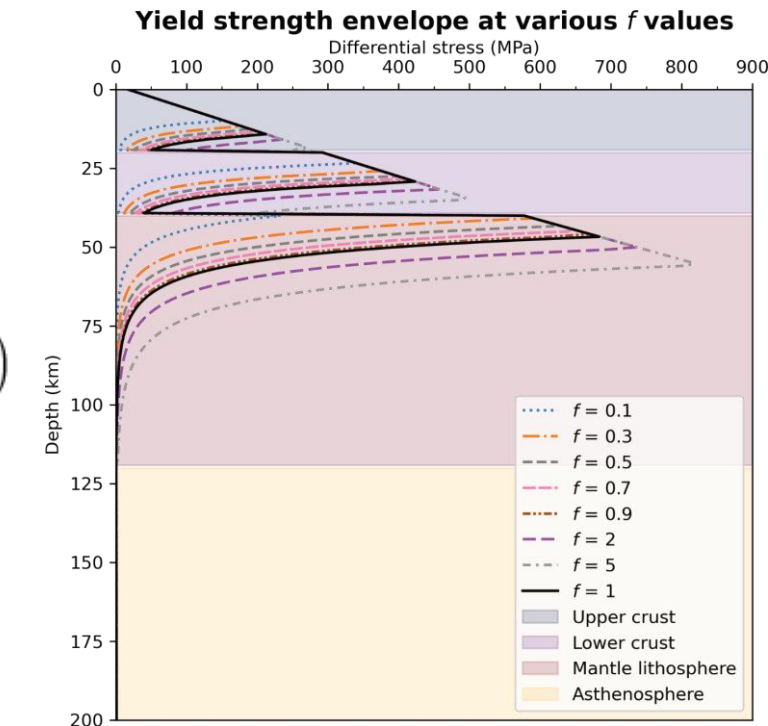
$$\sigma'_y = C \cos \phi + P \sin \phi$$

Given sufficient plastic strain, weaken cohesion C and angle of internal friction ϕ

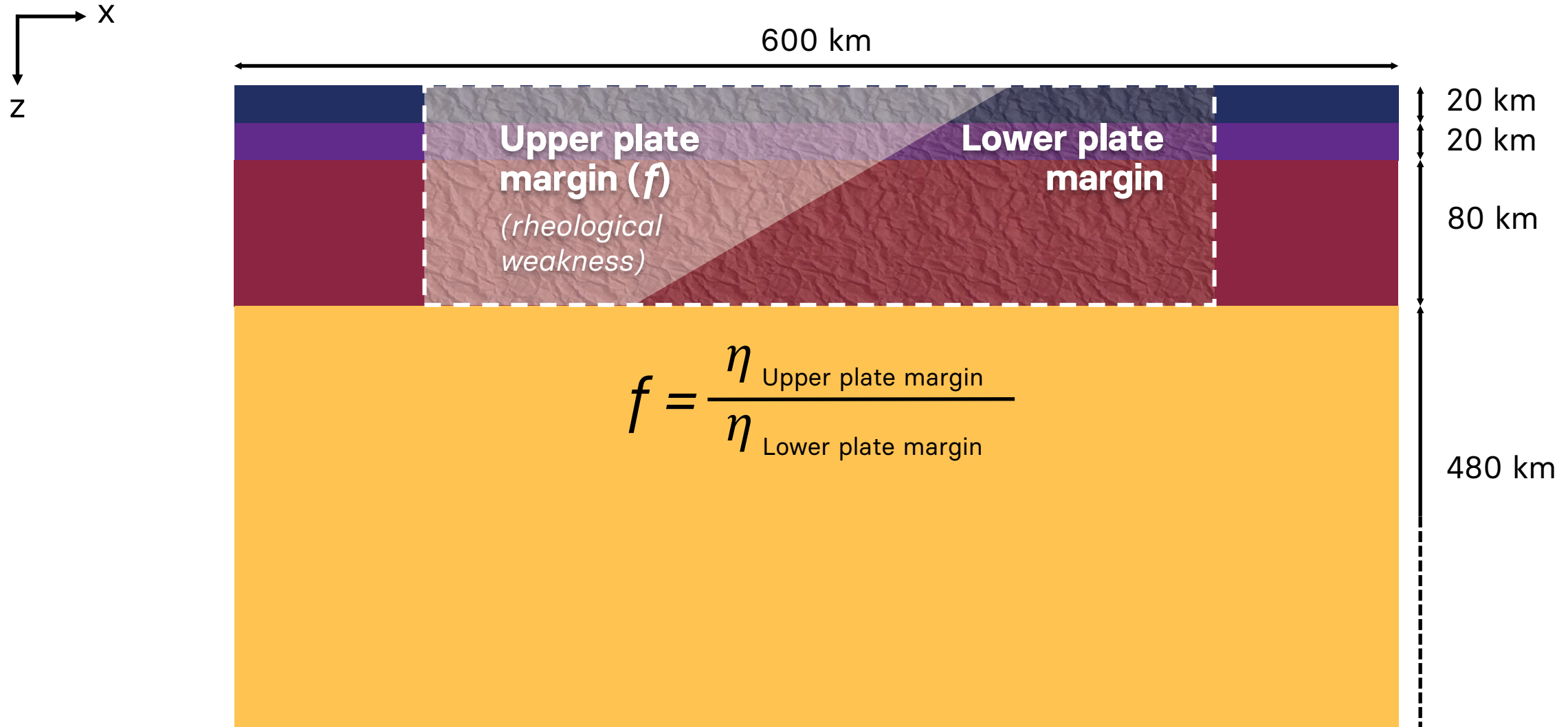


$$\eta = \frac{1}{2} A^{-\frac{1}{n}} d^{\frac{m}{n}} \dot{\varepsilon}_{ii}^{\frac{1-n}{n}} \exp\left(\frac{Q^* + PV^*}{nRT}\right)$$

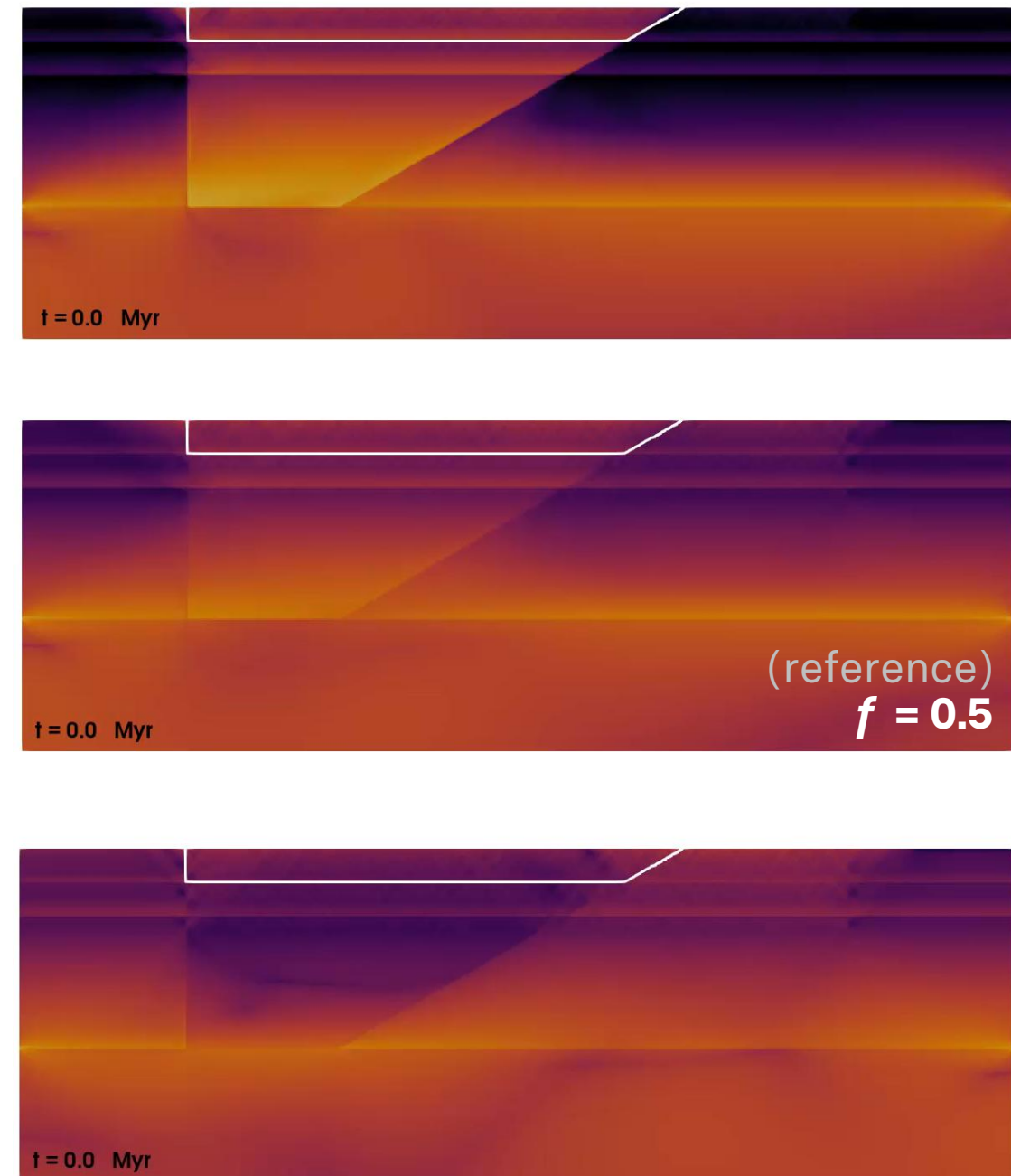
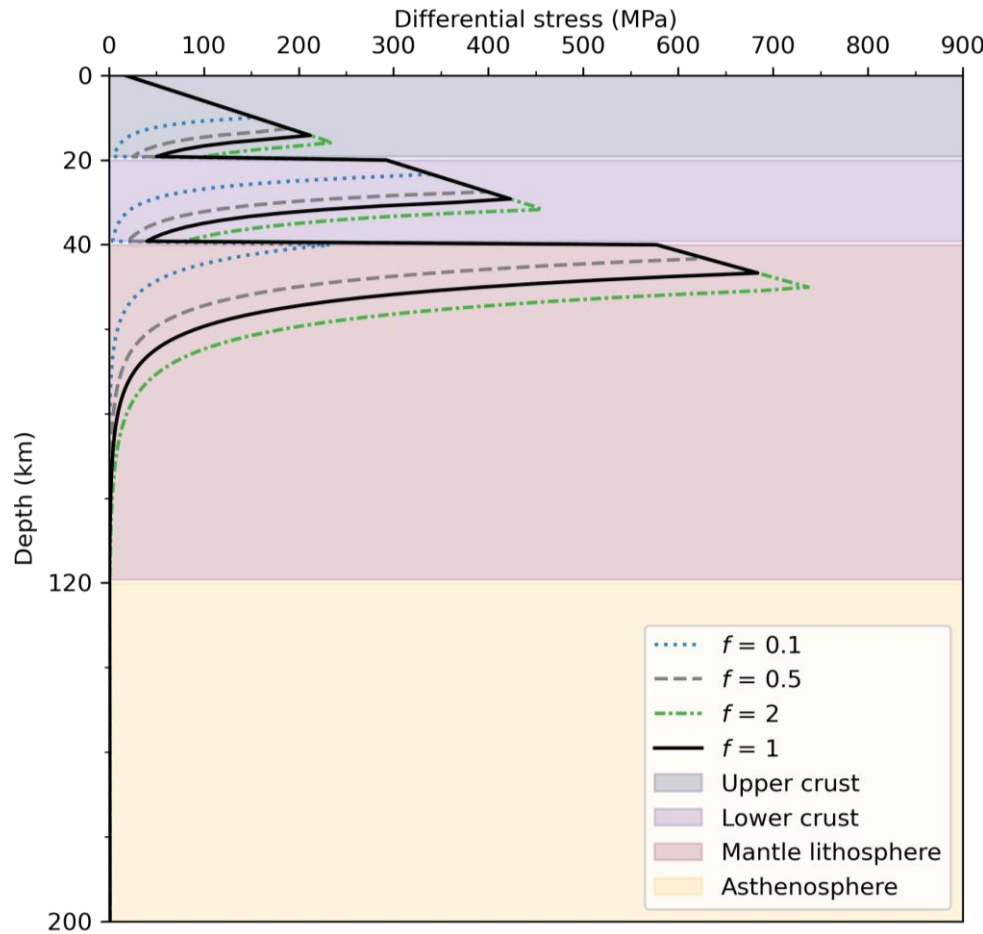
Scale effective viscosity by modifying material constant A



Strength parameter



Strength parameter



Strength parameter

- Changes the depth of brittle-ductile transition for the upper plate margin.
- $f = 0.1$ - delocalized thinning and long breakup.
- $f > 1$ - fragment forms in lower plate.

